Regional Precipitation Study in Central America, Using the WRF Model

Tito Maldonado

Using the regional climate model WRF, and the NCEP-NCAR Reanalysis Project data as boundary and initial conditions, regional precipitation was estimated by means of the dynamical downscaling technique for two selected periods, January 2000 and September 2007. These months show very particular climatic characteristics of the precipitation regimen in Central America, like dry (wet) conditions in the Pacific (Caribbean) coast of the Central American isthmus, in January, and wet (dry) conditions, respectively in each coast, during September. Four-nested-domains, each grids of resolution of 90 km (d01), 30 km (d02), 10 km (d03), and 3.3 km (d04), were configured over this region. The runs were reinitialized each 5 days with 6 hours of spin-up time for adjustment of the model. A total of 8 experiments (4 per month) were tested in order to study: a) two important Cumulus Parameterization Schemes (CPS), Kain-Fritsch (KF) and Grell-Devenyi (GD); and b) the physical interaction between nested domains (one- and two-way nesting), during each simulated month.

January 2000 results showed that the modeled precipitation is in agreement with observations, and also captured the mean climate features of rainfall concerning magnitude, and spatial distribution, like the particular precipitation contrast between the Pacific and the Caribbean coast.

Outputs from September 2007 revealed significant differences when a visual comparison is made to the spatial distribution of each coarse domain (d01, d02, and d03) with their respective domain in each experiment. However, the inner grids (d04) in all the experiments, showed a similar spatial distribution and magnitude estimation, mainly in those runs using one-way nesting configuration. Furthermore, the results for this moth differ substantially with observations, and the latter could be related with associated deficiencies in the boundary condition that do not reproduce well the transition periods from warm to cold El Niño episodes.

Moreover, in all the experiments, the KF scheme calculated more precipitation than the GD scheme and it is associated to the ability of the GD scheme to reproduce spotty but intense rainfall, and apparently, this scheme is reluctant to activate, frequently yielding little or no rain. However, when rainfall does develop, it is very intense.

Also, the time series do not replicate specific precipitation events, thus, the 5-days integration period used in this study, is not enough to reproduce short-period precipitation events.

Finally, physical interaction issues between the nested domains are reflected in discontinuities in the precipitation field, which have been associated to mass field adjustment in the CPS.

Uppsala universitet, Institutionen för geovetenskaper
Examensarbete E, 30 hp i Meteorologi
ISSN 1650-6553 Nr 244
Tryckt hos Institutionen för geovetenskaper,
Geotryckeriet, Uppsala universitet, Uppsala, 2012.

Regional Precipitation Study in
Central America, Using the WRF Model

Examensarbete vid Institutionen för geovetenskaper
ISSN 1650-6553 Nr 244

Tito Maldonado

Examensarbete vid Institutionen för geovetenskaper
ISSN 1650-6553 Nr 244

Regional Precipitation Study in Central America, Using the WRF Model

Tito Maldonado

Abstract

Using the regional climate model WRF, and the NCEP-NCAR Reanalysis Project data as boundary and initial conditions, regional precipitation was estimated by means of the dynamical downscaling technique for two selected periods, January 2000 and September 2007. These months show very particular climatic characteristics of the precipitation regimen in Central America, like dry (wet) conditions in the Pacific (Caribbean) coast of the Central American isthmus, in January, and wet (dry) conditions, respectively in each coast, during September. Four-nested-domains, each grids of resolution of 90 km (d01), 30 km (d02), 10 km (d03), and 3.3 km (d04), were configured over this region. The runs were reinitialized each 5 days with 6 hours of spin-up time for adjustment of the model. A total of 8 experiments (4 per month) were tested in order to study: a) two important Cumulus Parameterization Schemes (CPS), Kain-Fritsch (KF) and Grell-Devenyi (GD); and b) the physical interaction between nested domains (one- and two-way nesting), during each simulated month.

January 2000 results showed that the modeled precipitation is in agreement with observations, and also captured the mean climate features of rainfall concerning magnitude, and spatial distribution, like the particular precipitation contrast between the Pacific and the Caribbean coast.

Outputs from September 2007 revealed significant differences when a visual comparison is made to the spatial distribution of each coarse domain (d01, d02, and d03) with their respective domain in each experiment. However, the inner grids (d04) in all the experiments, showed a similar spatial distribution and magnitude estimation, mainly in those runs using one-way nesting configuration. Furthermore, the results for this moth differ substantially with observations, and the latter could be related with associated deficiencies in the boundary condition that do not reproduce well the transition periods from warm to cold El Niño episodes.

Moreover, in all the experiments, the KF scheme calculated more precipitation than the GD scheme and it is associated to the ability of the GD scheme to reproduce spotty but intense rainfall, and apparently, this scheme is reluctant to activate, frequently yielding little or no rain. However, when rainfall does develop, it is very intense.

Also, the time series do not replicate specific precipitation events, thus, the 5-days integration period used in this study, is not enough to reproduce short-period precipitation events.

Finally, physical interaction issues between the nested domains are reflected in discontinuities in the precipitation field, which have been associated to mass field adjustment in the CPS.

Keywords: WRF, Central America, precipitation, dynamical downscaling, regional models, reanalysis, cumulus parameterization schemes.

Resumen

Se utilizó el modelo regional WRF, y los datos del proyecto de reanálisis de NCEP/NCAR como condiciones iniciales y de frontera, para estimar precipitación a escala regional por medio de la técnica de reducción de escala (downscaling) dinámica, durante dos periodos seleccionados, Enero 2000 y Septiembre 2007. Estos meses presentan características climáticas particulares del regimen de lluvias en América Central, como condiciones secas (húmedas) en la costa Pacífico (Caribe), durante Enero, y condiciones húmedas (secas) respectivamente en cada costa, durante Septiembre. Cuatro dominios anidados fueron configurados sobre América Central, cada uno con una resolución de 90km (d01), 30 km (d02), 10 km (d03) y 3.3 km (d04). Las simulaciones fueron reinicializadas cada 5 días, considerando un periodo de 6 horas para ajuste del modelo (spin-up). Un total de 8 experimentos (4 por mes) fueron analizados con el objetivo de estudiar: a) dos esquemas de paramatrización de cúmulus (EPC) importantes, Kain-Fristch (KF) y Grell-Devenyi (GD), y b) la interacción de los procesos físicos entre los dominios anidados.

Los resultados de los experimentos de Enero 2000 muestran que la precipitación modelada coincide con las observaciones, y que además, captura las principales características climáticas, tanto, en magnitud como en la distribución espacial como el contraste presente entre las costas Pacífico y Caribe de América Central.

Las salidas de los experimentos de Septiembre 2007, muestran discrepancias cuando se comparan visualmente, la distribución espacial de precipitación en los dominios de baja resolución (d01, d02 y d03), con sus respectivos dominios en cada experimento. Sin embargo, en el domino interno (d04) de cada, no se encontraron mayores diferencias en la distribución espacial de lluvia, principalmente en aquellos experimentos en los que se utilizó retroalimentación dinámica en una dirección (one-way nesting). Por otra parte, los resultados de este experimento difieren considerablemente con las observaciones. Esto último podría estar relacionado con deficiencias en las condiciones de frontera, reflejadas en la representación de la transición de eventos cálidos a fríos de El Niño Oscilación del Sur.

En términos generales, el esquema KF calculó más precipitación que el esquema GD en todos y es asociado a que el esquema GD produce precipitación irregular, pero intensa, siendo reacio a activar, por lo que frecuentemente produce poca o nada de lluvia. Sin embargo, cuando la lluvia se desarrolla es muy intensa.

Además, las series de tiempo no capturaron eventos específicos, lo cual indica que el periodo de integración (5 días) utilizado no es el idóneo para reproducir eventos de corta duración.

Por último, se encontraron problemas de interacción física entre los dominios anidados, reflejados en discontinuidades en el campo de precipitación, los cuales son asociados a ajustes en el campo de masa de los EPC.

Palabras Clave: WRF, América Central, precipitación, reducción de escala dinámica, modelos regionales, esquemas de parametrización de cúmulus.

Referat

Nederbörden i Central Amerika har uppskattats med dynamisk nedskalning för två utvalda perioder, januari 2000 och september 2007. Global återanalysdata från NCEP-NCARs återanalysprojekt har använts som randdata och initialdata till den regionala klimatmodellen WRF. De studerade månaderna uppvisar stora variationer i nederbördsmönster, t ex lite (mycket) nederbörd under januari och mycket (lite) nederbörd under september för kustområdena längs Stilla havet (Karibiska havet). Fyra nästlade domäner över Central Amerika har använts med en upplösning på 90 km (d01), 30 km (d02), 10 km (d03) och 3,3 km (d04). Simuleringarna initialiserades var 5:e dag och de första 6 timmarna efter varje initialisering används för modellens anpassning till initialtillståndet. Totalt 8 experiment genomfördes (4 för varje månad) för att studera: (a) två olika sätt att parameterisera konvektion i Cumulusmoln (CPS), Kain-Fritsch (KF) och Grell-Devenyi (GD) och (b) den fysikaliska interaktionen mellan de nästlade domänerna (en- respektive tvåvägs nästlade scheman).

För januari 2000 var det god överensstämmelse mellan modellerad och observerad nederbörd. Modellen beskriver väl såväl mängden nederbörd som den rumsliga fördelningen, t ex den stora kontrasten mellan kustområdena längs Stilla havet och Karibiska havet.

För september 2007 uppvisar den modellerade nederbörden stora skillnader i de olika experimenten för de yttre domänerna (d01, d02, d03). För den inre domänen (d04) är resultaten från de olika experimenten betydligt mer lika, särskilt för experimenten med envägs nästlade scheman. Vidare skiljer sig den modellerade nederbörden väsentligt från observerad nederbörd under september 2007. Detta kan förklaras med felaktiga randdata på grund av problemet i återanalys data att reproducera perioder med övergång från varm till kall El Niño. I alla experiment gav KF mer nederbörd än GD, det kan förklaras med att GD bättre reproducerar kortvarig, intensiv nederbörd. Det finns en viss tröghet innan nederbörden i GD aktiveras, vilket innebär större frekvens av lite eller ingen nederbörd. När nederbörden väl utvecklas blir den dock intensiv. WRF-modellen klarar inte av att återge specifika nederbördshändelser för de genomförda experimenten, vilket betyder att 5-dagar är för lång simuleringstid för att kunna reproducera specifika händelser. Slutligen, interaktion mellan de nästlade domänerna skapar diskontinuiteter i nederbördsmönstren längs ränderna på domänerna, detta kan förklaras med justeringar av massfältet i CPS.

Nyckelord: WRF, Centralamerika, nederbörd, dynamiska nedskalning, regionala modeller, reanalys, cumulus parametrisering system.

Content

List of Tables

List of Figures

1. Introduction

The Central America isthmus is located in an area especially prone to natural disasters. This region has one of the highest frequencies of flooding and associated risks due to tropical cyclones (Alcántara-Ayala 2002). In agreement with this information, Alfaro et al. (2010) found that more than 70% of the natural disaster reports, in this region, are related to hydro-meteorological events. Floods and landslides registered more than 40% of the casualties owed to natural disasters. They also found that most of the event reports are from May to November, coinciding, with the rainy season in the Pacific slope and the hurricane season in the North Atlantic Ocean region (Alfaro 2002; Taylor and Alfaro 2005).

For instance, between 1961 and 2001, 10 large-scale hurricanes resulted in 18 816 dead, 3 783 279 displaced, and almost 14 billion US dollars in economic losses (Manuel-Navarrete et al. 2007). Furthermore, each year hundreds of small and mesoscale events provoke, together, more damages and disruption than most large-scale events.

It is thus clear that the study of the precipitation, and its variability is a necessity for governmental and non-governmental entities (Donoso and Ramirez 2001; Garcia-Solera and Ramirez 2012), and one of the major challenges for the scientific community (Enfield and Alfaro 1999; Magaña et al. 1999; Alfaro 2002, 2007, Maldonado and Alfaro 2010b, 2011).

For climatology studies of the atmosphere or any meteorological variable, data from either meteorological stations or results of Numerical Weather Prediction (NWP) models can be used. On the one hand, observations can be employed to study the climate and its variations over time in a specific region. Furthermore, observations can be used to validate the outputs and/or calibration of NWP models. Nonetheless, some requirements must be satisfied to use observed data such as long time series, and, if it is possible, a good spatial resolution (stations network). Besides that, a quality control must be applied to assure reliability of such information. Unfortunately, in Central America, the lack of databases with such characteristics is one of the main claims of the scientific community. See for example recent works such as Morales Méndez (2010), Quesada Montano (2011), and Reynolds (2012).On the other hand, the use of mesoscale models rises as an alternative to study weather and climate of any particular region (Amador and Alfaro 2009). These models, also known as Regional Climate Models (RCMs) or Local Area Models (LAMs), are based in the physical and dynamical principles of the fluids (Warner 2010). LAMs downscale the information generated by General Circulation Models (GCMs, Trenberth 2010), which have a resolution typically of 150 - 300 km, to resolutions in between 10 - 50 km, or even less (Mass et al. 2002). This method is known as dynamical downscaling. Thus, LAMs can be used to build weather prediction systems and for climate research (Warner 2010). An added value is that these models capture topographical details that are not represented in GCMs, and give additional information in regions with deficiency of measurements. Yet, there is still uncertainty associated to the lack of climatic data for verification of the models (Washington and Parkinson 2005; Trenberth 2010). Thus, it is recommended an adequate knowledge of the climate of the region of interest to be able to use LAMs (Amador and Alfaro 2009).

However, experimentation using mesoscale models in Central America has been scarce (Hernandez et al. 2006; Rivera and Amador 2009; Maldonado and Alfaro 2010a). These previous studies employed the MM5 model (Grell et al. 1994; Dudhia et al. 2012), to study climate features in the region. They noticed that this RCM had a good performance simulating dynamical variables like the horizontal wind field, and thermo-dynamic variables such as temperature, but, precipitation results have shown some discrepancies.

Thus, the aim of this work is to study precipitation as a result of dynamical downscaling, using the mesoscale Weather Forecast and Research model (WRF, Skamarock et al. 2008) in Central America. Two months, January 2000 and September 2007, will be simulated, which represent two important phases of the precipitation regime in this area (Magaña et al. 1999). Furthermore, due to the importance of the convective processes in local and regional scale circulations in the tropics, two cumulus parameterization schemes (CPS), will be studied. Such CPSs have been often used to estimate convection implicitly in mesoscale models. Also, some issues found related to the physical interaction among nested domains will be addressed.

This work is structured as follows. In Section 2 some climate features of the precipitation in Central America are described, Section 3 discusses about the downscaling techniques, and some advantages and disadvantages of each technique are given. Section 4 exposes the problem to study, and in Section 5 the methodology for this analysis is explained, Section 6 shows the results, and, finally, Section 7 presents a discussion of the results and in Section 8 a summary and conclusions of this study are presented.

2. Precipitation climatology in Central America

2.1 The annual cycle

The topography and location of Central America have an important role in the spatial and temporal distributions of rainfall during the year. High mountains divide the isthmus in two main climate regions, the Pacific and the Caribbean sides, located in lee and windward respectively, according to the North Atlantic trade winds, which is the dominant wind regime (Maldonado et al. 2012, submitted manuscript). These slopes show a dramatic contrast in the annual distribution of rainfall (Magaña et al. 1999). Thus, different mechanisms for rainfall production can be working in those regions.

The annual cycle of precipitation in the Pacific coast presents a bimodal precipitation distribution, with maxima in May-June and in September-October, and relative minimum during July-August (Magaña et al. 1999, Taylor and Alfaro 2005; Amador et al. 2006). This reduction has been termed by Magaña et al. (1999) as the mid-summer drought (MSD). The first maximum occurs due to the pole ward migration of the Inter Tropical Convergence Zone (ITCZ), thus, during May-June the rainy season begins. Besides that, the Sea Surface Temperature (SST) of the neighboring oceans exceeds 29 °C, and deep convection activity is developed along with a sub-tropical lower-tropospheric cyclonic circulation anomaly over the subtropics. During July-August the convective activity diminishes, due to a decrease of

SST of about 1 °C, the cyclonic circulation anomaly weakens, corresponding to an anticyclonic acceleration of the low-level flow and, therefore, to an intensification of the trade winds over Central America, when the MSD occurs. This leads to a formation of divergence anomalies that inhibit deep convection activity, and the strengthening of the easterlies, forcing upward motion and intense precipitation over the Caribbean side, and subsidence and clear skies upon the Pacific slope.

The second peak occurs during August through October due to the presence of fewer deep clouds, which would produce an increment of incoming solar radiation heating the SST above 28 °C. Then, this warming in the SST produces an increase of water evaporation from the oceans to the atmosphere; in addition, weakened trade winds and a low-level convergence anomaly lead to enhanced deep convection. Normally, this season presents the highest frequency of extreme events over the Pacific slope (Maldonado et al. 2012, submitted manuscript). While in the Caribbean coast, rainfall decreases during these months, owed to a decrease in the strength of the trade winds (Taylor and Alfaro 2005; Amador et al. 2006). Moreover, this season also has the highest probability of hurricane occurrence over the North Atlantic Ocean and Caribbean Sea (Alfaro et al. 2010). From December to March, the Pacific slope of Central America presents warm and mostly dry conditions. During these moths, the ITCZ is at its southernmost position (Amador et al. 2006). In the Caribbean side, precipitation during the winter months is mostly related to the mid-latitude air intrusions (Schultz et al. 1997, 1998), and to less frequent low-level cloud systems traveling from the east (Velasquez 2000).

2.2 Influence of regional scale circulation systems

Two important dynamical features that modulate the weather and climate in the region appear during summer and winter. The first mechanism is the Intra-Americas Low-Level Jet (IALLJ, Amador 2008) over the Caribbean Sea. It is developed during May-June, and reaches its maximum in July and weakens in September (Amador 1998; Amador and Magaña 1999; Amador et al. 2000;. 2003; Amador 2008). It is barotropically unstable, and has potential interaction with transients, such as easterly waves. In this sense, the IALLJ may feed energy to the easterly waves, which then increase their meridional amplitude to the north of their mean position, as they travel westward across Central America and southern Mexico, and into the eastern tropical Pacific region (Amador et al. 2006).

From May till July, easterly waves loose energy and momentum strengthening the mean current and causing the low-level jet to peak in July. From September till early November trades winds are relatively weak, vertical wind shear over the Caribbean is reduced, hurricane activity peaks, and rainfall spreads almost all over The Gulf of Mexico, The Caribbean Sea, and the eastern tropical Pacific adjacent to southern Mexico, Central America, and northwestern South America. On late November or early December, trades increase again, cold surges start to reach the tropics, and a second maximum of wind appears over the Caribbean Sea.

These features make the IALLJ an important element to explain the convective activity during July through November, and contribute to understand the climate of the region, but they are not applicable to winter months (December, January and February), when the IALLJ reaches a peak in February when no major tropical wave activity is observed (Amador 2008).

The IALLJ crosses Central America through the mountain gaps and reaches the easternmost region of the tropical Pacific. Some surges associated to synoptic-scale events have been associated with strong wind-topography interaction and precipitation on the Caribbean slope of Central America.

The core intensity of the IALLJ varies with El Niño Southern Oscillation (ENSO) phases in such way that during warm (cold) events the jet core is stronger (weaker) than normal in the boreal summer, surface wind stress and wind stress curl area expected to be stronger (weaker) than normal in the easternmost portion of the eastern tropical Pacific. Contrary to what happens in summers, the jet core is weaker (stronger) than normal during warm (cold) ENSO phases in winter (Amador 2008).

The second mechanism is the Chocó low-level jet (Poveda and Mesa 2000), in the western coast of Colombia near 5 °N. It reaches its maximum by October-November, then decreases its intensity until being almost absent during the period February-March. Low-level warm air and moisture convergence associated with the Chocó Jet, low surface pressure and orographic vertical motion on the western Andes, contribute to deep convective activity, which is organized as mesoscale convective complexes. The Chocó jet differs with the IALLJ in: the latter is at least twice stronger than the former. This may implies that their origin and maintenance are linked to quantitatively different momentum sources (Amador et al. 2006). Furthermore, the Chocó jet, in contrast to the IALLJ, is not barotropically unstable. The Colombian jet varies as well with ENSO episodes, but, out of phase compared with its Caribbean jet counterpart. During warm (cold) ENSO phases the Chocó jet presents weaker (stronger) than normal wind speeds (Poveda and Mesa 2000), being the opposite pattern to the one showed by the IALLJ.

2.3 The time evolution of SST and its influence on the precipitation field

The influence of the SST anomalies in the precipitation variability field has been widely studied (Enfield and Alfaro 1999; Alfaro 2000, 2007). In these investigations the beginning and ending of the rain spells are related to fluctuations in the SST of the Atlantic and Pacific Oceans, and, these anomalies are related to the magnitude of rainfall and frequency of rainy days (Maldonado and Alfaro 2010b, 2011; Maldonado et al. 2012, submitted manuscript).

Amador et al. (2006) point out that the seasonal cycle of SST is important in defining key climatological features, especially during summer-autumn, such as the Western Hemisphere warm pool (WHWP) development (Wang and Enfield 2001; Wang and Fielder 2006), the appearance of MSD (Magaña et al. 1999), and favorable areas for cyclogenesis (Banichevich and Lizano 1998; Goldenberg et al. 2001). During the northern winter, SST isotherms over the Caribbean and the eastern tropical Pacific are mostly zonally distributed,

with values usually below 28-29 °C, except in the central eastern tropical Pacific, and to the west of Central America, where there is a maximum of SST all year. As result of this, and a relatively strong vertical trade wind shear, and reduced evaporation, no major convective activity occurs in most of the Pacific coast of Central America during this season. Also, during boreal winter, the ITCZ is at its southernmost position (Srinivasan and Smith 1996). During boreal summer, a large warm pool dominates the SST distribution over most of the eastern tropical Pacific region (da Silva et al. 1994; Magaña et al. 1999, Wang and Enfield 2001, 2003). In the Caribbean warm pool, organized activity is barely observed, due mainly to strong vertical wind shear (Amador et al. 2000), and strong subsidence associated with regional scale circulations, such as those associated with the low-level jet described above.

The eastern tropical Pacific deck/cold tongue/ITCZ complex has a large annual cycle (Croning et al. 2002). From February through April equatorial waters over this region area warms, trade winds are weak, and upwelling is reduced. Cool equatorial water, stratus clouds extending to the equator, strong trade winds and deep convection reaching Central America are characteristics of this ocean-atmosphere complex from August through October (Amador et al. 2006).

2.4 Other tropical rain-producing systems

As mentioned above, during warm (cold) ENSO phases, the IALLJ shows stronger (weaker) than normal wind speeds (Amador et al. 2000, 2003, 2006; Amador 2008). This fluctuation are reflected in SST anomalies over the Caribbean Sea, north of Venezuela coast; a strong (weak) jet results in negative (positive) SST anomalies over this region due to strong (weak) Ekman transport. In this way, the jet may have a role in coupling SST anomalies in eastern Pacific during El Niño or La Niña events with anomalies over some regions of the Caribbean during summer. Variations in surface variables (precipitation and temperature) in different sectors of Mesoamerica, including its west coast, are the result of a combination of fluctuations in the equatorial tropical Pacific and in the tropical north Atlantic/Intra-Americas Sea region (Amador et al. 2006). Studies as Alfaro et al. (1998), Alfaro and Cid (1999a,b), and Enfield and Alfaro (1999), found that the strongest rainfall signal occurs when tropical north Atlantic and tropical Pacific SST anomalies are in a configuration of meridional dipole (antisymmetric) across the ITCZ, that is, when this anomalies have an opposite sign. The rainy season in south Central America tends to start early and end late in years that begin with warm SST in the tropical North Atlantic. Ending dates are also delayed when the eastern tropical Pacific is cool.

Another type of disturbance that contributes to precipitation in Central America is the “temporales” (Hanstenrath 1991). They are periods of weak-moderate nearly continuous rain, lasting several days and affecting a relatively large region. Their definition includes the condition that wind must be weak; however, Amador et al. (2003) have shown that in some cases winds can be intense and long-lasting. The frequency of these events presents a great deal of interannual an intraseasonal variability, and their relationship to ENSO or to other large-scale climatic signal is still unclear (Amador et al. 2006). These

perturbations are not only associated with the Pacific ITCZ, but also related to westward-traveling, low-level cloud system over the Caribbean reaching the Pacific, which are not necessarily associated with mid-latitude cold air intrusions (Velásquez 2000).

3. The dynamical downscaling approach

One solution to the lack of observations is the use of GCMs. These models can generate reliable information for authorities, decision-makers and scientists. They employ the complete set of dynamical equations to study atmospheric processes at global scale. They use a geometrical computational domain of the globe employing some spatial and temporal representation of the variables (finite difference and/or spectral methods), and, mostly, including implicitly small-scale processes in the equations (Holton 2004). GCMs have a general representation of the climate of any region; thus, they do however have a poor representation of local climate features due to their coarse resolution, typically 150 – 300 km. Because of this problem, to generate information at local or regional scales (10 to 50 – 60 km), two approaches are commonly used – interpolation methods and downscaling techniques. These methods have advantages and disadvantages, which will not be discussed here, but some comparison can be found in Amador and Alfaro (2009). However, two aspects should be highlighted; first, the statistical relations are not causality relations implying less ability for description and understanding of the physics and dynamics of the interactions among the climate system elements. These statistical relations must be sustained by a conceptual physical model. Second, downscaling has the potential to generate climate scenarios taking into account regional spatial variations and the interaction among the climate system elements. The latter approach can use statistical or dynamical methods. Nowadays, both statistical and dynamical downscaling, have shown good skill for prediction of the atmospheric variables, under the same climate conditions (Gershunov et al. 2000; Wilby and Dawson 2004).

Therefore, on the one hand, the statistical downscaling can generate information from GCM outputs to either station or regional scale and in different temporal scales – daily, monthly or seasonal scales. Any statistical downscaling scheme uses empirical relationships among the predictors (large scale variables) and the predictants (local or regional scale variables). These methods have some advantages such as they require a low computational cost, and sometimes the relations between predictor-predictant are non-stationary (Wilby and Dawson 2007), simulating better the real behavior of the climate system (Amador and Alfaro 2009). However, this approach requires a good quality of observed time series for the calibration. Furthermore, the results are dependent in the selection of the predictors, and the empirical transfer functions. On the other hand, the dynamical downscaling uses the Local Area Models (LAMs) or Regional Climate Models (RCMs) which are known as mesoscale models. This approach generates high resolution information from the GCM outputs. RCM can employ sub-regional domains of few kilometers (10 – 50 km), but associated uncertainty could be expected due to increase resolution, and less understanding of physical processes. There is evidence that these models simulate better the regional

climate and meteorology than GCMs (Giorgi and Mearns 1999), and, especially over mountains, important issue in the spatial domain in Central America (Amador and Alfaro 2009). Furthermore, RCMs incorporate the state-of-the-art of the physics and dynamics of the climate system, and can simulate adequately the interaction among the elements of the climate system. But, in spite of their great potential, RCMs require a high computational power, good knowledge of the climate of the region, and experience using climate models.

4. Aim of this research

The general objective of this research is to study precipitation using the dynamical downscaling technique with the WRF model. The representation of seasonal patterns in the model is also studied. To achieve this, two months (January 2000, and September 2007) are simulated. Comparisons between the Pacific and the Caribbean sides of Central America are made to determine whether the model is capable to reproduce the spatial distribution of precipitation during those months.

As part of this analysis, a comparison between two cumulus parameterization schemes (CPS) is made, in order to detect whether the model results are sensible in the inner grids to changes in the physical representation of the cumulus convection. Finally, the study of the physical interactions among nested domain is carried out with the interest to analyze what issues imply to use one- or two-way nesting, related to magnitude, and, spatial distribution of rainfall calculated by the model.

5. Methodology

The mesoscale model WRF version 3 (Skamarock et al. 2008) is used. This model is a Numerical Weather Prediction (NWP) designed for both research and operational applications. It has been widely used in other tropical regions around the world, for instance Davis et al. (2008), Ray et al. (2011), and Vaidya (2007), showed good results in precipitation estimation.

This model has some important characteristics such as: (a) a fully compressive set of equations; (b) Euler non-hydrostatic with a run-time hydrostatic option available; (c) prognosis variables such as horizontal velocity (u,v) in Cartesian coordinates, vertical velocity (w), and perturbation of potential temperature; (d) the vertical coordinate system is terrain-following, dry hydrostatic-pressure with vertical grid stretching allowed; and (e) top of the model is a constant pressure surface; (f) for horizontal grid the Arakawa C-grid staggering is used.

Furthermore, it allows performing one-way interactive, two-way interactive and moving nests. For physics, it employs microphysics schemes ranging from simplified physics to sophisticated mixed-phase physics suitable for process studies and NWP. Also, it uses cumulus parameterization with adjustment and mass-flux schemes for mesoscale modeling. Multi-layer land surface models from simple thermal model to vegetation and soil moisture models are used for surface physics. Non-local K schemes are used to parameterize physics in the planet boundary layer, and longwave and shortwave schemes with multiple spectral

bands and a simple shortwave scheme suitable for climate and weather prediction applications.

5.1 Experimental design

Two months, January 2000, and September 2007 were chosen to simulate regional precipitation in order to study the WRF performance in downscaling applications. These months have some particular features described as follows. Climatologically, on January the dry season is already set upon the Pacific slope, whereas the Caribbean side in contrast, shows wet conditions. By September, the Pacific coast is wetter than the Caribbean coast. Furthermore, during this month there is a high probability of occurrence of extreme events of precipitation (Alfaro et al. 2010; Maldonado and Alfaro 2010b, 2011).

However, since in this research, two specific periods are simulated, it is important to have a look of the meteorological condition reported during those months. Through the first case, the meteorological report states that cold episode (La Niña) conditions prevailed in the Pacific throughout 2000, continuing the long-running episode that began in mid-1998. This cold episode conditions were reported as strongest during 2000-01 Northern Hemisphere winter season (Lawrimore et al. 2001). Locally, in Central America, normal conditions during La Niña events were reported: cold maximum temperatures below normal values, and surplus of precipitation over the Caribbean side. According to National Meteorological Service of Costa Rica (IMN 2000), during January 2000, migrating high pressure systems (>1030 hPa) from Gulf of Mexico to Caribbean Sea produced trade wind with moderate to high velocities. Cold air intrusion from North America with relative periodicity provoked a decrement in maximum temperatures (about 3 °C) in San Jose, Costa Rica. The southern Caribbean part of Central America was the most affected by the intrusion of cold fronts that reached such latitudes. In the Caribbean coast of Costa Rica the monthly accumulated observed was 468 mm, that is, more than 100 mm with respect to the monthly mean value (308 mm). While the Pacific side, the monthly accumulated recorded by the stations was catalogued as normal.

During the second case, the year 2007 was characterized by a transition to La Niña condition, developed until August, resulted in suppressed convection near the date line by early June. Also, the Atlantic hurricane season was near normal, and slightly more active than in 2006. Tropical cyclone activity was significantly below average in the eastern North Pacific (Levinson and Lawrimore 2008). At regional scale, the National Meteorological Service of Costa Rica (IMN 2007) reported during this month (2007), extreme precipitation events mainly in the central and north part of the country. The monthly accumulated in this area was of the order of 400 mm. In this region several natural disasters like floods were also recorded. Stations located in the Pacific and Caribbean side of the country reported rainfall below normal. Furthermore, 9 tropical cyclones were developed in the Caribbean basin, of which 3 became in hurricanes. Just Felix was an intense hurricane; nevertheless, it had no affectation over the country due to the anticyclone circulation, and a disorganized ITCZ.

5.1.1 DOMAIN CONFIGURATION

Figure 1a shows the four-nested-domain configuration upon Central America used in this study. The selected resolutions from the outer to the inner domains are 90, 30, 10 and 3.3 km. The size and resolution of the outer grids (d01) were chosen to decrease the interpolation effects from the boundary conditions (Warner 2010). Furthermore, it should be noted this area enclosed an important part of both ocean called the Western Hemisphere Warm Pool. (Wang and Enfield 2001, 2003; Enfield et al. 2006; Lee et al. 2007; Wang et al. 2008a,b). As mentioned in Section 2, the SST of this oceanic region has an important influence in the timing and duration of the precipitation over Central America (Enfield and Alfaro 1999; Alfaro 2000, 2007; Maldonado and Alfaro 2010b, 2011). Other mesoscale phenomena within this domain are the cold air intrusions from the northern hemisphere due to frontal zones (Schultz et al. 1997, 1998), and the easterly waves, which are important mechanisms for rainfall production during January and September, respectively (Amador et al. 2006).

The domains d02 and d03 are selected to smooth the information flowing from the outer to the inner domain d04. Besides, this configuration is aimed to avoid some topographical forcing at the boundaries, and it is aimed to enclose the whole Central America region in a domain with resolution of 3.3 km. Figure 1 also shows the topography in outer (Fig. 1b) and inner (Fig. 1c) domains. Notice the enhancement in representation of the topographical features in the inner domain. Also, 28 vertical levels were configured in the mesoscale model.

The NCEP/NCAR Reanalysis Project data (Kalnay et al. 1996; Kistler et al. 2001) were used as boundary and initial condition. This model has a horizontal resolution of 2.5°, and a output frequency of 6 hours. Simulations were reinitialized each five days rather than attempting continuous simulations, following the results from Qian et al. (2003), and Rivera and Amador (2009), in which they showed that short period simulations, in contrast to continuous runs, have the smallest error in precipitation compared to observations. Furthermore, 6 hours of spin-up time for adjustment of the model is considered in agreement with Wang and Seaman (1997), and Rivera and Amador (2009). Wang and Seaman (1997) found that during the first 6 hours the model shows inability to handle precipitation forecasts.

5.1.2 PHYSICAL PARAMETERIZATIONS

First, all domains use CPS but one, the inner grids only uses an explicit convection scheme. The latter is following the recommendations given by Molinari and Dudek (1992). They found that for a grid spacing that falls below 5-10 km, an explicit scheme is enough to represent cumulus convection, but it cannot provide a general solution for resolutions above 10 km. A hybrid approach, allowing explicit and implicit schemes, works better for grid spacing greater than 10 km (mesoscale models), since this method separate convective-scale motions from the slow growth, fallout, and phase changes of detrained hydrometeors that produce mesoscale organization of convection. The cumulus schemes tested were

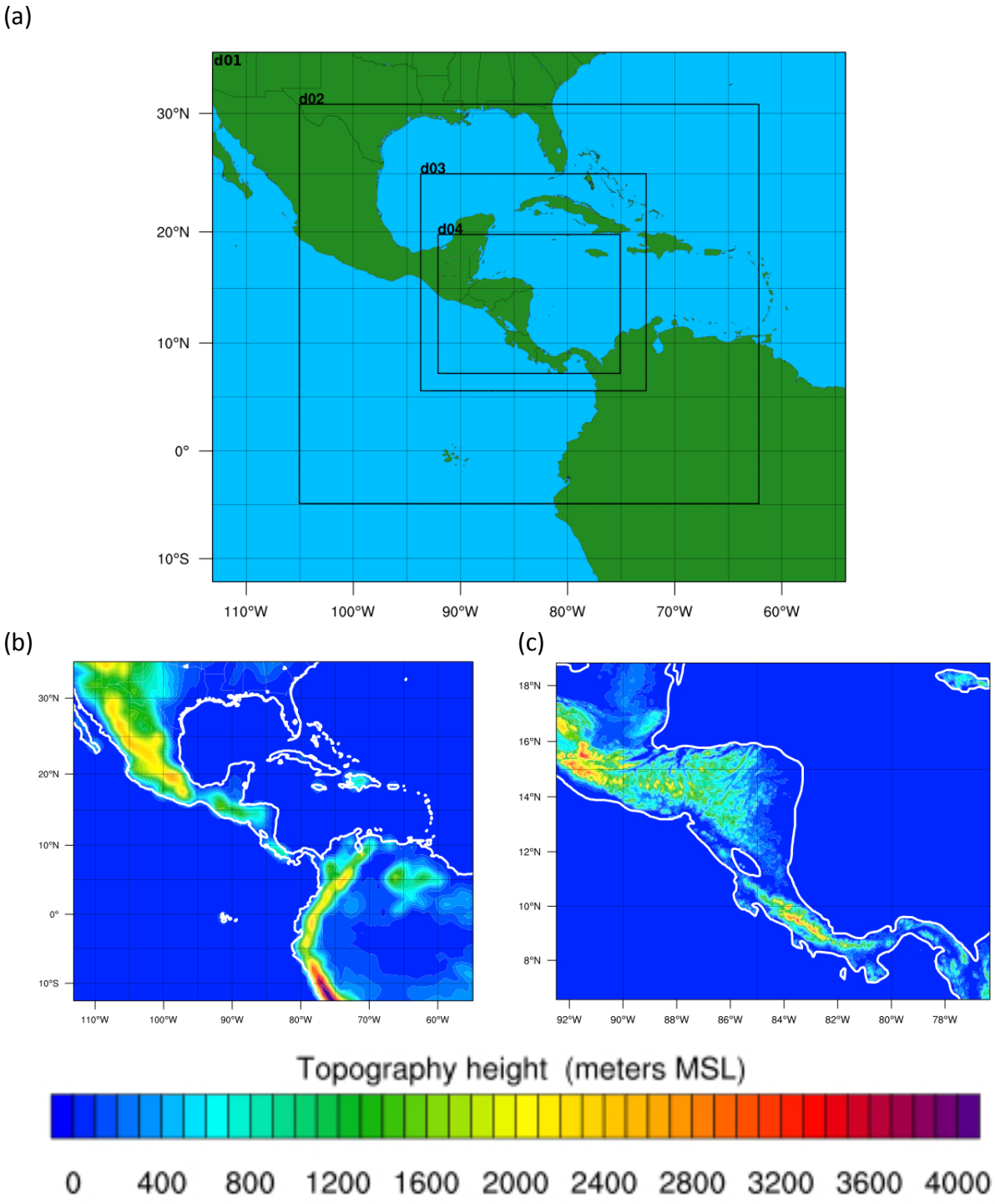

Figure 1. Area coverage for the computational domains (grids) (a) 1, 2, 3 and 4; topography for (b) 1 and (c) 4.

Grell-Devenyi (GD, Grell and Dévényi 2002), and Kain-Fritsch (KF, Kain 2004). Those schemes have been widely used in other studies such as Bukovsky and Karoly (2009), Maldonado and Alfaro (2010a), Warner et al. (2003), Rivera and Amador (2009), Wang and Seaman (1997).

GD introduce an ensemble cumulus scheme in which effectively multiple cumulus schemes and variants are run within each grid box and then the results are averaged to give

feedback to the model. The schemes are all mass-flux type schemes, but the updraft and downdraft entrainment and detrainment parameters, and precipitation efficiencies differ. These differences in static control are combined with differences in dynamic control, which is the method to determine cloud mass flux. The dynamic control closures are based on convective available potential energy (CAPE), low-level vertical velocity or moisture convergence.

The KF scheme is based on Kain and Fritsch (1990, 1992), but has been modified based on testing within the Eta model. It utilizes a simple cloud model with moist updrafts and downdrafts, including the effects of detrainment, entrainment, and relatively simple microphysics. The current KF scheme differs from the original KF scheme in the following ways: (a) a minimum entrainment rate is imposed to suppress widespread convection in marginally unstable, relatively dry environments; (b) shallow (non-precipitating) convection is allowed for any updraft that does not reach minimum cloud depth for precipitating cloud, varying as a function of the cloud-base temperature; (c) the entrainment rate is allowed to vary as a function of low-level convergence; and (d) downdraft changes such as the source layer, mass flux as a fraction of updraft mass flux at the cloud base and detrainment is specified to occur in updraft source layer and below.

Other physical parameterization schemes considered in this research were: (a) for microphysics the WRF single-moment 6-class (WSM6) was chosen. This scheme includes graupel and associated processes. It uses a new method for representing mixed-phase particle fall speeds for the snow and graupel particles by assigning a single fall-speed to both that is weighted by the mixing rations, and applying that fall-speed to both sedimentation and accretion processes (Dudhia et al. 2008); (b) for shortwave radiation the MM5 scheme is used. This scheme is based on Dudhia (1989) in which has a simple downward integration of solar flux, accounting for clear-air scattering, water vapor absorption, and cloud albedo and absorption; (c) Land-Surface physics uses the Pleim-Xiu LSM scheme (Pleim and Xiu 1995; Xiu and Pleim 2001), includes a 2-layer force-restore soil temperature and moisture model. The top layer is taken to be 1 cm thick, and the lower layer is 99 cm. This scheme features three pathways for moisture fluxes: evapotranspiration, soil evaporation, and evaporation from wet canopies; (d) Surface physics scheme employs similarity theory MM5, and it uses stability functions to compute surface exchange coefficients for heat, moisture and momentum; and (e) Planet Boundary Layer (PBL) uses the Medium Range Forecast Model (MRF) described by Hong and Pan (1996). It employs a counter-gradient flux for heat and moisture in unstable conditions. It uses enhanced vertical flux coefficients in the PBL, and the PBL height is determined from a critical bulk Richardson number. It handles vertical diffusion with an implicit local scheme, and it is based in the local Richardson number in the free atmosphere. The so-called first-order local-*K* approach following Louis (1979) is used for boundary layer as well as the free atmosphere.

Finally, runs allowing no interaction (one-way nesting) or interaction (two-way nesting) among domains were performed. Table 1 shows a summary of the experimental design in this research.

Table 1. Cumulus parameterization schemes (CPS), feedback option and notation used for the experiments.

CPS	Feedback	Month	Experiment
KF	On	January 2000	KF2WJ00
KF	Off	January 2000	KF1WJ00
GD	On	January 2000	GD2WJ00
GD	Off	January 2000	GD1WJ00
KF	On	September 2007	KF2WS07
KF	Off	September 2007	KF1WS07
GD	On	September 2007	GD2WS07
GD	Off	September 2007	GD1WS07

5.2 Description of the methods for verification of the model outputs

Daily precipitation data from meteorological gauge stations are used for verification of the model outputs. Such data base has been widely used in other precipitation studies such as Maldonado and Alfaro (2010b, 2011), Quesada-Montano (2011), Maldonado et al. (2012, submitted). These data were gathered by the Center for Geophysical Research (Centro de Investigaciones Geofísicas, CIGEFI, in Spanish), University of Costa Rica. After a quality control, taking stations with at least 60% of the data during each month, a total of 92 and 48 stations left in January and September, respectively. These stations were divided in three regions in order to capture important precipitation structures, and due to its quality.

Figure 2 displays the stations used for each case. Notice the deficit of stations in September 2007 compared to January 2000. This reduction in number of stations was also noted in Quesada Montano (2011, her figure 2), and she explained that this reduction is produce by two reasons: 1) A number of stations of the network have been out of service, and 2) Obtaining reports from some of these stations has been increasingly difficult.

From each model domain, the nearest grid points to station were compared. The same statistical methods described in Pierce et al. (2009) are used here. These authors evaluate a broad spectrum of metrics based on temperature and precipitation for a selection of models. In the present work, only precipitation is analyzed. The following metrics will be applied to the spatial distribution.

Let the model output be $m(\mathbf{x})$ and the observations be $o(\mathbf{x})$. The mean squared error (MSE) in $m(\mathbf{x})$ is defined as

$$MSE(m,o) = \frac{1}{N}\sum_{k=1}^{N}(m_k - o_k)^2$$

where there are N spatial points. Then, a dimensionless spatial skill score (SS) is defined by normalizing

(a) (b)

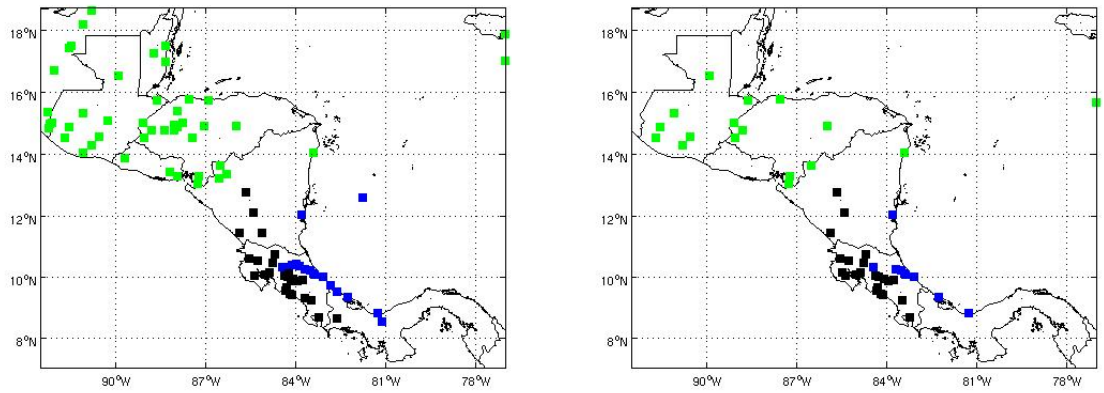

Figure 2. Spatial distribution of meteorological stations deployed in Central America during (a) January 2000 and (b) September 2007. Blue squares represent stations located in southern Caribbean, 17 in (a), and 9 in (b); black squares are stations in south Pacific, 27 in (a), and 22 in (b); green squares are stations in northern Central America, 48 in (a), and 17 in (b).

$$SS = 1 - \frac{MSE(m,o)}{MSE(\bar{o},o)}$$

A model output identical to observations has a skill score of 1. It was normalized by $MSE(\bar{o},o)$ where the overbar indicates the spatial mean; in this case, represents the monthly accumulated average for all statistics. A completely featureless, uniform pattern yields a spatial skill score of 0. This skill score can be decomposed as:

$$SS = r_{m,o}^2 - \left[r_{m,o} - s_m/s_o\right]^2 - \left[(m-o)/s_o\right]^2$$

where $r_{m,o}$ is the product moment spatial correlation coefficient between the model and observations, and s_m and s_o indicate the sample standard deviation of the model and observations, respectively. The right-hand terms are described as follows: the first term is the square of the correlation, and is a measure of the proportion of the variability that is accounted for by the forecast. The second term is the conditional bias, and expresses the degree in which a spatial regression between the model and observations has a slope that differs from the unity. The third term is the square of the unconditional bias, as a fraction of the standard deviation of the observations. The sense of this decomposition is that the skill starts from the square of the correlation, and, is penalized for any conditional of unconditional bias.

6. Results

6.1 January 2000 case

Figure 4 shows the daily average rate of precipitation during January 2000 in domain d01 (90km). This figure illustrates the relaxation zone in the boundaries of the domain. This pattern was also noted in Bukovsky and Karoly (2009). Furthermore, both experiments KF1WJ00 and KF2WJ00 show unrealistic results approximately in between 10-12 S and 75-70W. Stensrud et al. (1995), and Gochis et al. (2002), found using an older version of KF scheme same non-physical spots, and they explain that such unrealistic intense bands of precipitation are located right at the upwind boundary where unstable air from the coarse domain enters the finer-grid domain. There is an inflow at this boundary, and the thermodynamic structure of the imported atmosphere is largely determined by the structure on the coarse domain, that in this case, NCEP/NCAR reanalysis uses the Arakawa-Schubert convective scheme developed by Pan and Wu (1994). Also, notice that this region is close to high mountains – the Andes, which could intensify these instabilities due to orographic effects.

(a) (b)

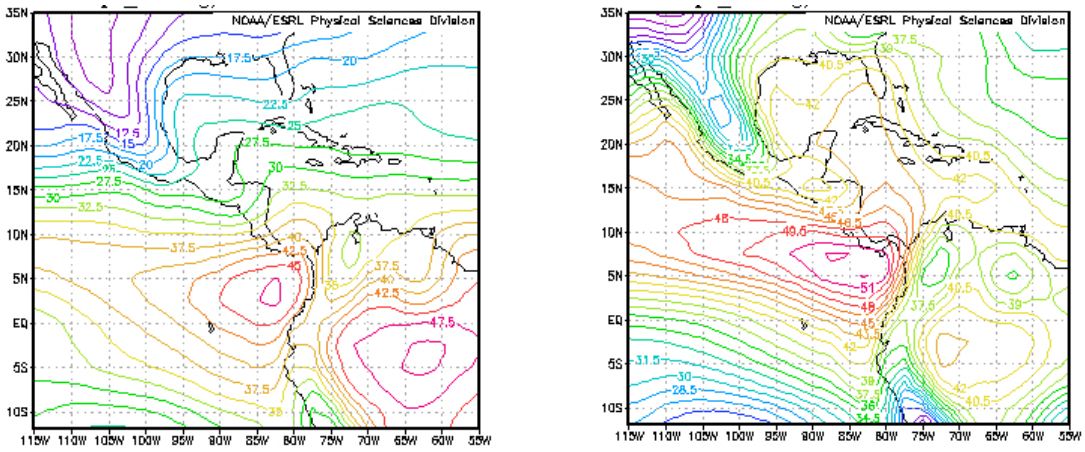

Figure 3. NCEP/NCAR daily average of precipitable water for (a) January 2000, and (b) September 2007. The isoline spacing is: (a) 2.5 kgm^{-2}, and (b) 3.0 kgm^{-2}.

Three important high precipitation regions are also showed in Figure 3a, and b, also noted in NCEP-NCAR reanalysis outputs (Figure 4); the first one over the northeast coast of Brazil (less intensity), a second one is positioned towards the center of South America. The third one and largest is located close to the western coast of Colombia, where the Chocó low-level jet is developed (Poveda and Mesa 2000). According to these authors, this region is known as the rainiest area of the Americas, and arguably in the world. In this region, normally during the quarter December-January-February the average of precipitable water is 45-50 mm/day (See their Fig. 5). The amount of rainfall calculated in KF2WJ00 case, was

40-50 mm/day being physically plausible. The amount calculated in KF1WJ00 test was 20-30 mm. The experiments GD2WJ00 and GD1WJ00 detected this maximum, but with less intensity, underestimating it considerately, 16-20 mm and 18 mm, respectively, compared to the climatology. Another important feature of Figure 4 is the relative maximum of rainfall present over the Caribbean coast of Nicaragua and Costa Rica, and the drier conditions detected in the Pacific side. Such a contrast has been already documented, and it is one of the major climatic features of the precipitation during the boreal winter (Amador et al. 2006). Among the dynamical mechanisms that explain that pattern are the interaction between northeasterly cold winds intrusions during this month and the topography. Also, in Figure 4 the ITCZ is located in between 5-15 N. In general, KF2WJ00 (GD1WJ00) predicts more (less) rainfall than the rest of experiments.

Figure 5 and 6 show the average daily rate of precipitation in grids 2 and 3, respectively. Since these grids were used to smooth the information flow from the outer to the inner domain, some general aspects will be commented. The experiments KF2WJ00 and KF1WJ00, in both figures, show the largest amount calculated by the model, consistently with the previous results in the outer domain. Maximum over the west coast of Colombia, and the Caribbean side of south Central America are detected in both grids, but notice that the amount differs in each case. From these graphs, one can see that GD1WJ00 case do not reproduce the same intensity these maxima, mainly over the continental part of Nicaragua and Costa Rica.

From these maps (Fig. 5 and 6), in the experiments KF2WJ00, and GD2WJ00 discontinuities in the precipitation field were found. In these domains (grids 2 and 3) a hybrid convection scheme (explicit and implicit) was employed. These discontinuities coincide with the boundaries of the inner domain, in which only an explicit convection scheme was allowed. Notice that in these cases, feedback among the nested domain was allowed. Same irregularities in the precipitation field were found first by Warner and Hsu (2000) using the MM5 model, and lately by Bukovsky and Karoly (2009) using the WRF and Amador (2012) [Amador, J. A., 2012. Personal Communication]. The latter gives evidence that there are physical interactions issues present in the convection schemes, which are not model dependent. Such discontinuities appear to be due to the mass adjustment in inner grids, which are influenced through the propagation of gravity waves across their boundaries, causing unreal attenuation or increase convection (Warner and Hsu 2000).

In inner grids (Fig. 7), only an explicit convection scheme is permitted. One can see from this figure, in the Caribbean side a rainfall maximum that extends over the east coast of Costa Rica, and northern Panama, and decreases towards southern Nicaragua. Nevertheless the position and amounts of this maximum differ considerately between the experiments. The KF experiments calculate more precipitation than experiments using GD. The north Caribbean side seems to be drier than south. Same structure was found in grids 2 and 3 (Fig. 5 and 6, respectively).

Monthly precipitation accumulated was estimated for stations located within the area 9.5-10.5N, 82.5-86W, and for their respective, nearest grid-point in each model domain (Fig. 8). Such distribution of the stations was chosen in order to study the rainfall structure, mainly in south Central America commented in Section 2. Observations and grids detected

the same contrast – low (high) rainfall in the Pacific (Caribbean) side. Notice that an increase in resolution seems to improve the precipitation output. In order to determine if both curves (observations and model outputs) come from the same distribution (null hypothesis); a Kolmogorov-Smirnov test (KS, Wilks 2005) was performed. According to Table 2, in inner grids of the GD2WJ00 and KF1WJ00 experiments the null hypothesis is accepted at the 95% of confidence level, but it is not accepted in the other two cases (KF2WJ00 and GD1WJ00).

Table 3 shows the statistical metrics calculated in the southern Caribbean area (blue squares Fig. 2a). This region is of special interest, because the observations and model detected heavy rain there. Best correlation and skill score are found in domain 4, in GD2WJ00 experiment. Although, the monthly accumulated of precipitation was underestimated about the 15% less than the monthly average (470 mm) reported by stations in this region, during January 2000. However, the unconditional bias gives evidence that such a value is smaller than the variability observed in the stations. Conditional bias (low value) indicates a linear relation between observation and forecast, confirmed by Figure 9b.

KF1WJ00 configuration shows also good results in grids 4, but here, the bias has a clear tendency to overestimate the precipitation as resolution gets finer. Furthermore, precipitation is overestimated about the 7% compared to the monthly average observed in the stations. Conditional and unconditional bias differs from the previous case, and a regression positive biased is detected in this case (Fig. 9c).

The other two cases (KF2WJ00 and GD1WJ00) are negatively biased. Notice also the configuration GD1WJ00 (Fig. 9d) tends to increase rainfall with resolution, but it is still underestimating precipitation in a large proportion, about 36% of the reported amount by the observations. Furthermore, scatter plots of that configuration show a big dispersion (Fig 9a).

South Pacific region (black squares Fig 2a, Table 4) exhibits high correlation, and skill scores – mainly in finer domains, nevertheless, the monthly precipitation accumulated is underestimated in the order of 50 mm, in this region (about 35% of the spatial average during this month).

North Central America (green squares Fig 2a, Table 5) has the worst results, low correlation, and negative skill score, besides that, precipitation is underestimated. However, the interpretation of these results should be done carefully, since the observations and model detected low precipitation there, mostly in north Central America.

Time series of the daily average accumulated of the stations, and grid-points (nearest to stations) located in south Caribbean region (blue squares in Fig. 2a) are shown in figure 10. This graph illustrates that the model do not represent specific events. In cases using two-way nesting, time series of each domain, tends to replicate the same time evolution. That pattern was not observed in one-way nesting cases. Time series were also done for stations in north and south Pacific (black and blue squares Fig. 2a), but results do not present any interesting remarkable feature due to low precipitation observed in the model and stations.

(a) KF2WJ00 (b) GD2WJ00

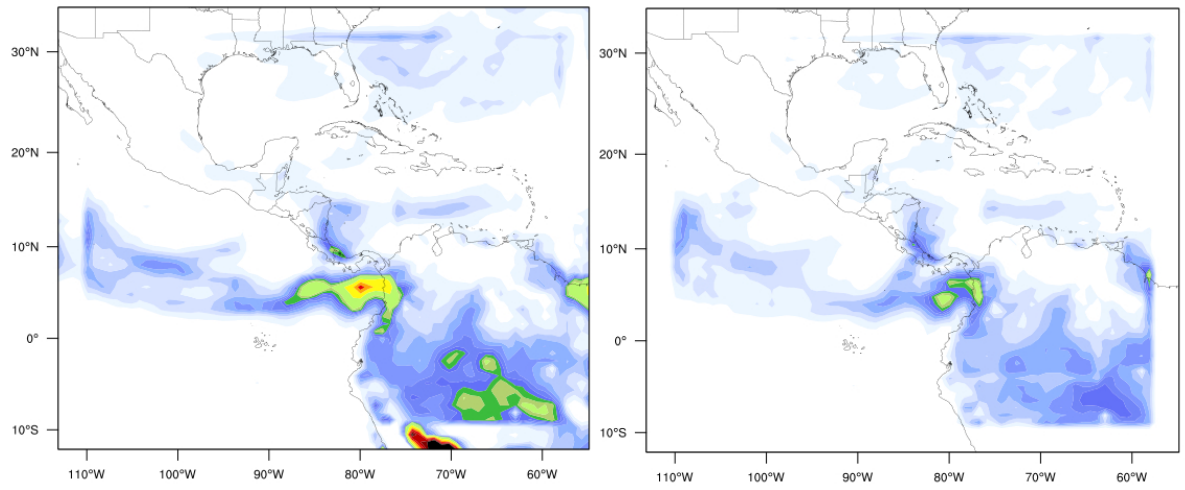

(c) KF1WJ00 (d) GD1WJ00

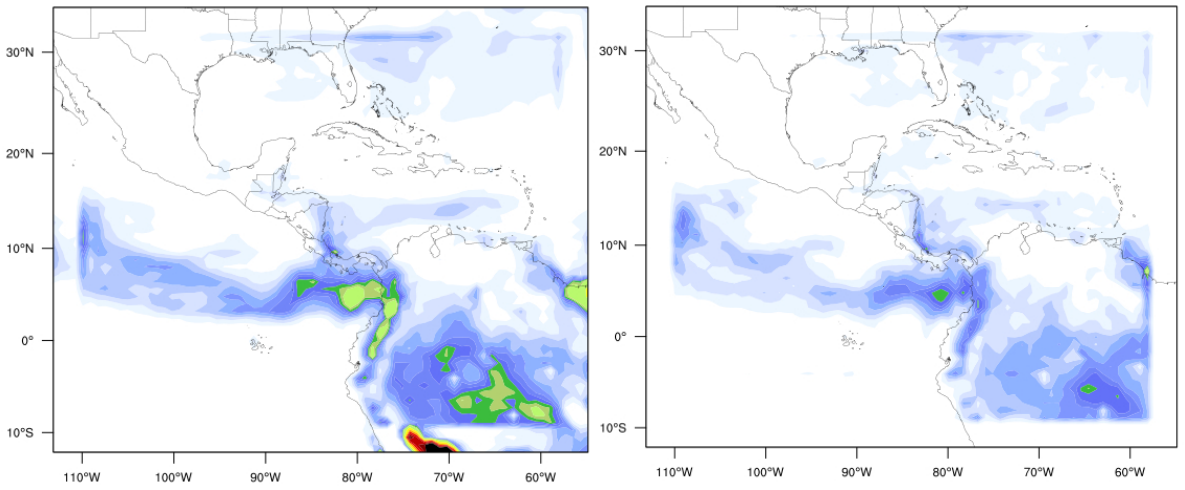

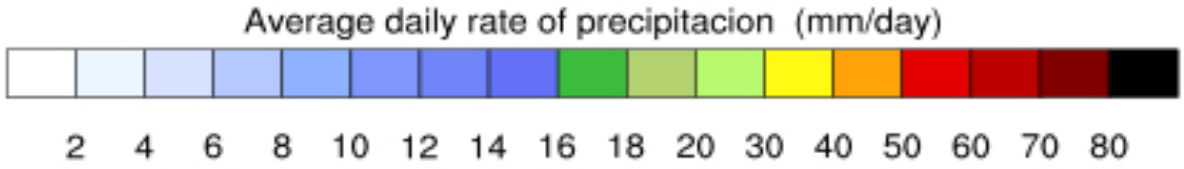

Figure 4. Outer grids (90km) in each experiment for January 2000 using (a) and (c) Kain-Fritsch (KF), and (b) and (d) Grell-Devenyi (GD). Also (a) and (b) use two-way nesting; (c) and (d) use one-way nesting for each scheme.

(a) KF2WJ00

(b) GD2WJ00

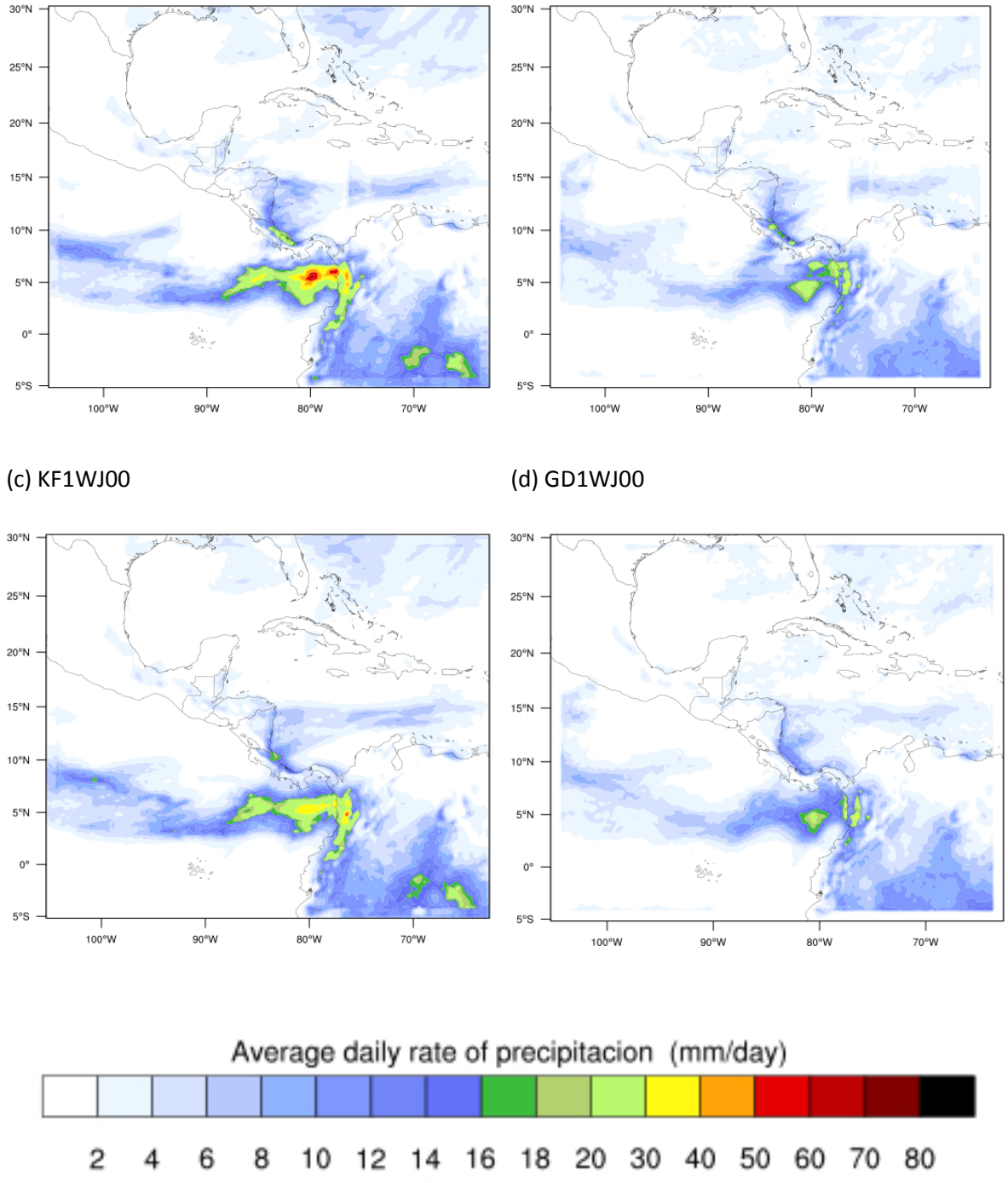

(c) KF1WJ00

(d) GD1WJ00

Figure 5. As in Fig. 4, but for domain 2 (30km).

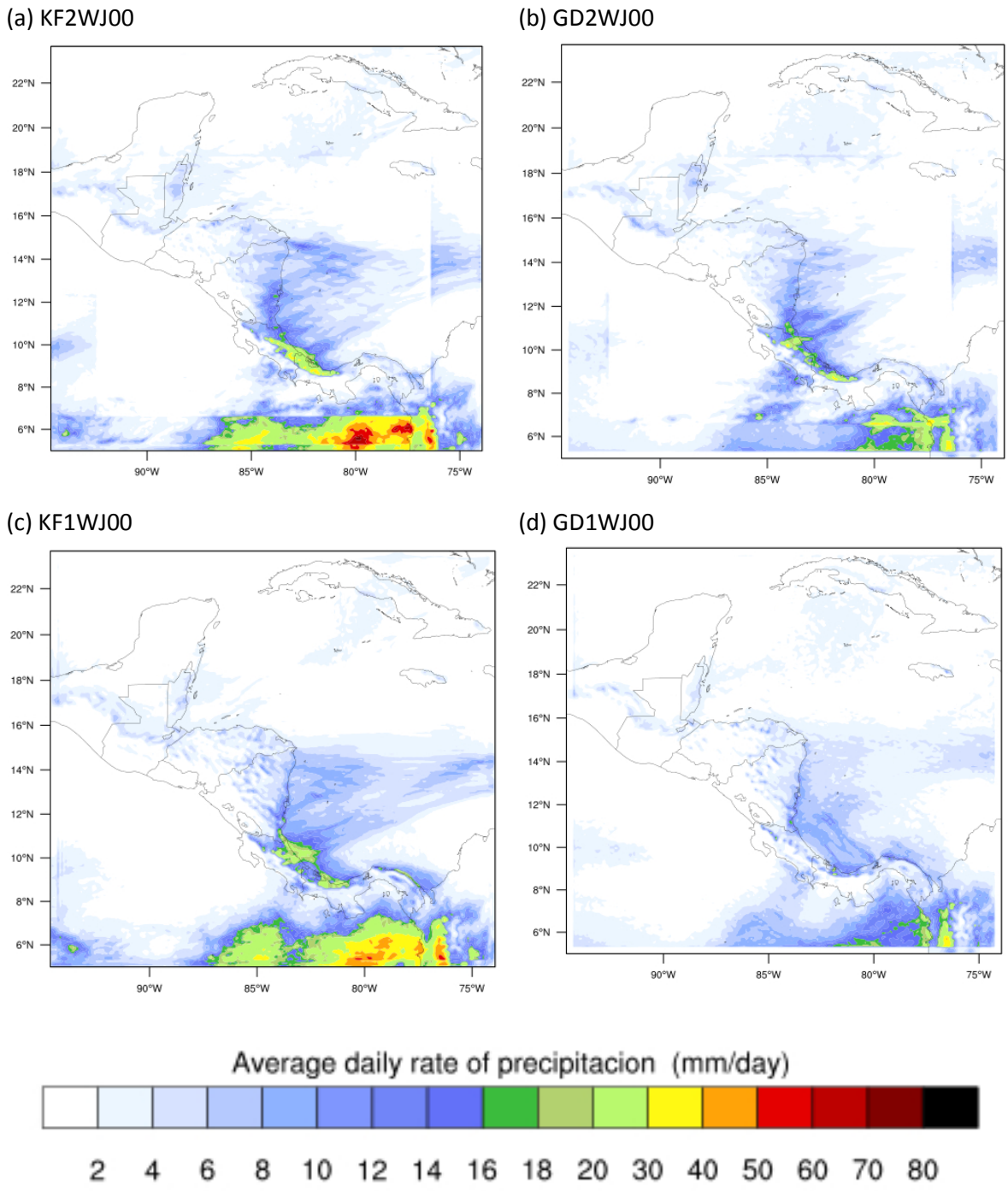

Figure 6. As in Fig. 4, but for domain 3 (10km).

(a) KF2WJ00 (b) GD2WJ00

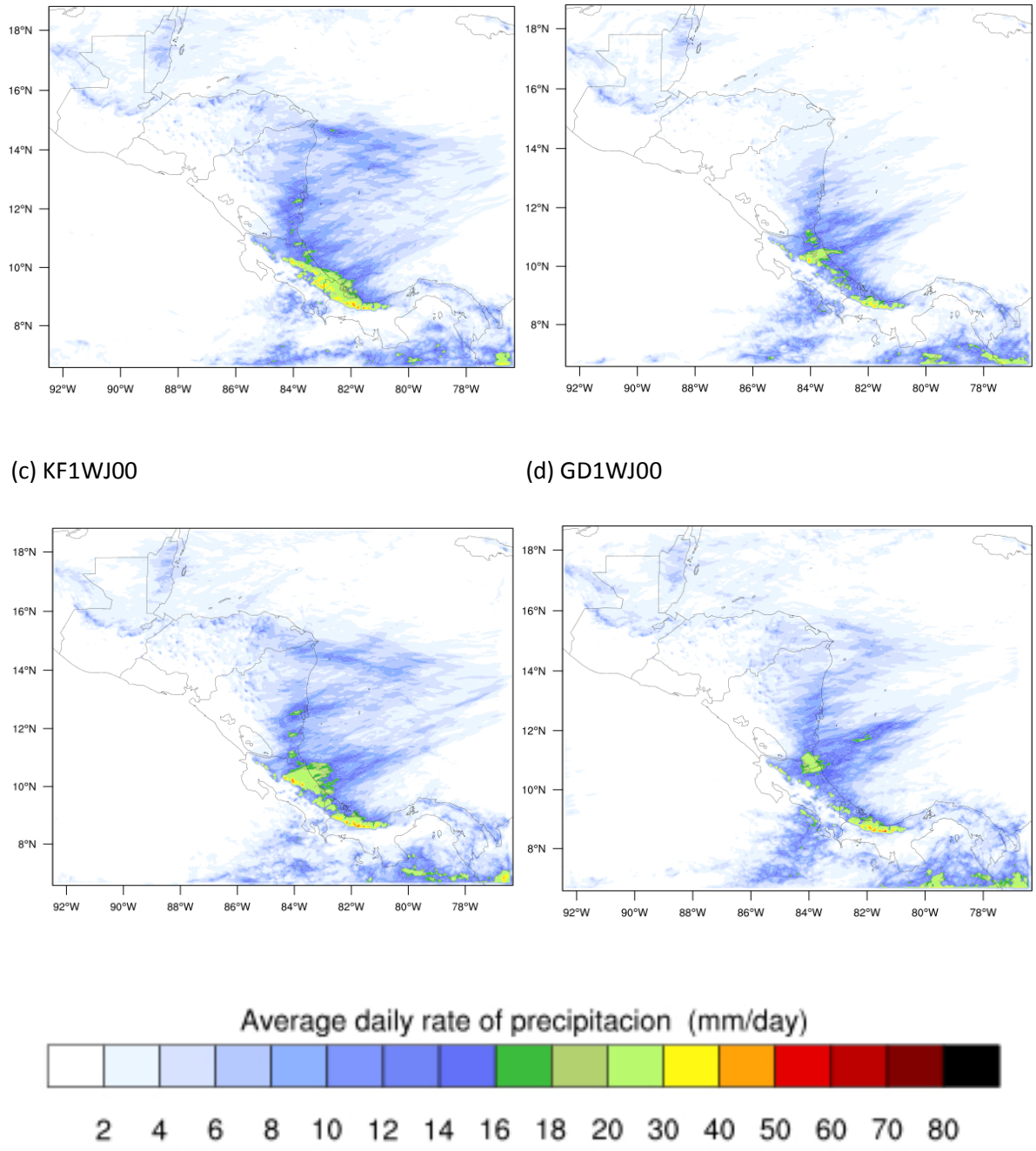

(c) KF1WJ00 (d) GD1WJ00

Figure 7. As in Fig. 4, but for domain 4 (3.3km).

(a) KF2WJ00

(b) GD2WJ00

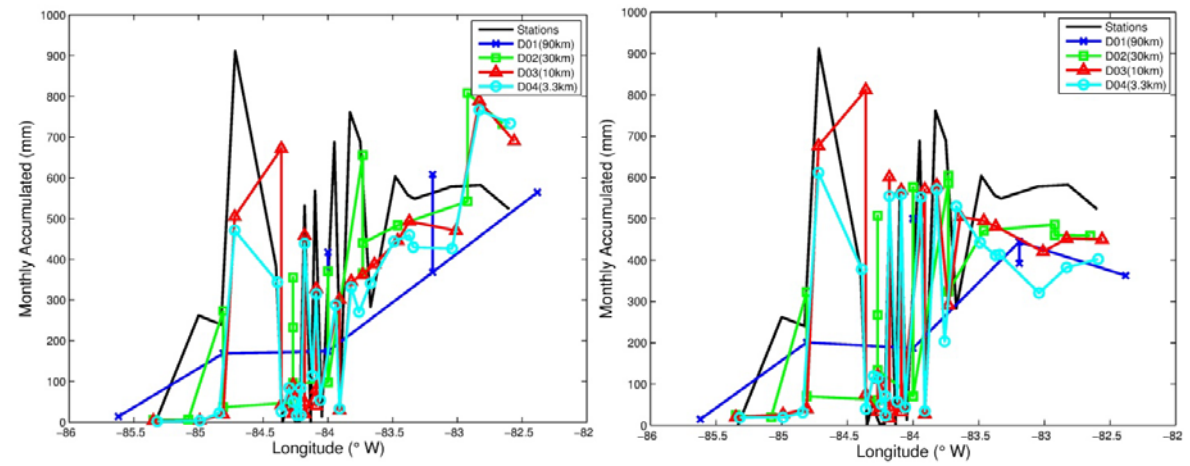

(c) KF1WJ00

(d) GD1WJ00

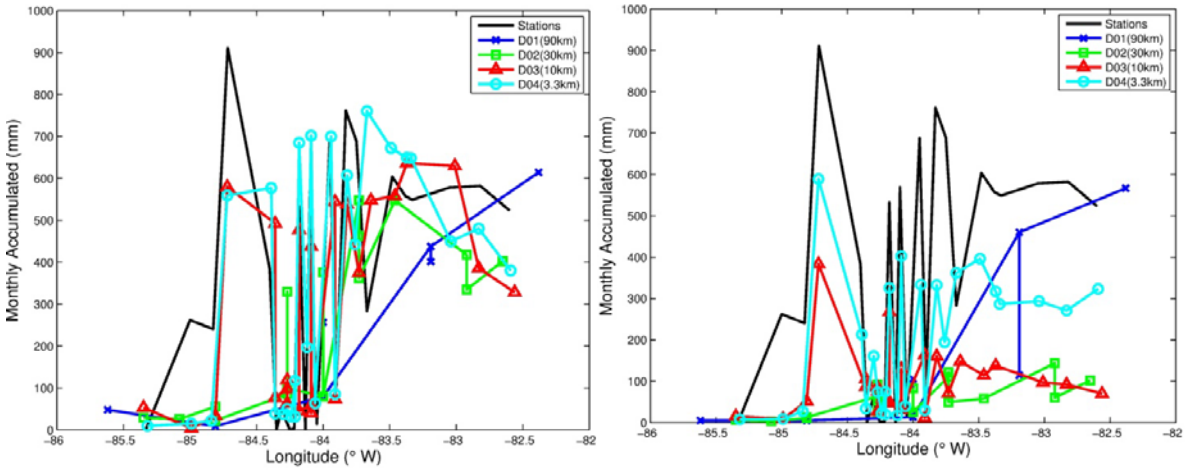

Figure 8. Monthly precipitation accumulated profiles of the stations and nearest grid-point in each domain, to the gauges within the area 9.5 – 10.5N, 82.5 – 86W, for January 2000.

Table 2. Kolmogorov-Smirnov test for two curves under the hypothesis that both come from the same distribution of data. The test was applied for the monthly precipitation accumulated profiles in Fig. 8. Numbers in bold are within the 95% of confidence level. P-values are in parenthesis.

	(a) KF2WJ00	(b) GD2WJ00	(c) KF1WJ00	(d) GD1J00
D01	**0.35(0.07)**	0.46(0.00)	0.42 (0.01)	0.50(0.00)
D02	**0.31(0.14)**	**0.31(0.14)**	**0.35 (0.07)**	0.65(0.00)
D03	**0.35(0.07)**	**0.23(0.44)**	**0.23 (0.44)**	0.58(0.00)
D04	0.38(0.03)	**0.23(0.44)**	**0.19 (0.67)**	0.42(0.01)

Table 3. Statistical results of each experiment (a) KF2WJ00, (b) GD2WJ00, (c) KF1WJ00 and (d) GD1WJ00. 470mm monthly average accumulated during January 2000 was reported by gauges located in south Caribbean zone (blue squares in Fig. 2a). These stations were compared with the nearest grid-point in each domain. Metrics shown here are the product-moment correlation (r), conditional bias (CB), unconditional bias (UCB), skill score (SS) and bias (B) as in Pierce et al. (2009).

(a)	d01	d02	d03	d04	(b)	d01	d02	d03	d04
r	0.52	0.27	0.37	0.45		0.75	0.70	0.62	0.78
CB	0.00	0.27	0.25	0.16		0.05	0.01	0.04	0.01
UCB	0.04	0.00	0.02	0.09		0.09	0.00	0.00	0.13
SS	0.22	-0.20	-0.14	-0.05		0.42	0.47	0.35	0.46
Bias	-42.54	-6.02	-31.73	-60.96		-61.65	-13.09	-13.94	-74.95
(c)					(d)				
r	0.19	0.64	0.72	0.69		0.00	0.00	0.19	0.72
CB	0.23	0.00	0.00	0.10		0.78	0.41	0.06	0.07
UCB	0.43	0.16	0.00	0.03		1.32	2.57	2.30	0.65
SS	-0.65	0.25	0.52	0.34		-2.18	-3.14	-2.47	-0.25
Bias	-135.53	-81.71	1.16	36.65		-238.10	-332.11	-314.56	-167.56

Table 4. As in Table 3 but for the south Pacific area (black squares in Fig 2a), and 141mm monthly average accumulated was reported by the stations.

(a)	d01	d02	d03	d04	(b)	d01	d02	d03	d04
r	0.04	0.68	0.88	0.85		0.14	0.69	0.86	0.83
CB	0.35	0.04	0.12	0.13		0.18	0.05	0.04	0.07
UCB	0.04	0.01	0.06	0.07		0.05	0.00	0.03	0.04
SS	-0.40	0.41	0.60	0.53		-0.21	0.42	0.67	0.58
Bias	45.77	-26.22	-52.49	-56.83		49.08	-13.52	-36.11	-45.98
(c)					(d)				
r	-0.13	0.10	0.64	0.82		-0.17	0.42	0.82	0.87
CB	0.09	0.00	0.09	0.06		0.35	0.00	0.06	0.08
UCB	0.27	0.24	0.11	0.04		0.05	0.06	0.02	0.03
SS	-0.36	-0.24	0.21	0.57		-0.38	0.11	0.59	0.64
Bias	-113.89	-106.30	-73.52	-44.52		-47.76	-51.92	-27.60	-40.40

Table 5. As in Table 3 but for the north Central America (green squares in Fig 2a), and 82mm monthly average accumulated was reported by the stations.

(a)	d01	d02	d03	d04	(b)	d01	d02	d03	d04
r	0.07	0.14	0.13	0.14		0.13	0.13	0.14	0.20
CB	0.10	0.12	0.12	0.11		0.04	0.09	0.10	0.04
UCB	0.09	0.05	0.06	0.08		0.14	0.09	0.11	0.16
SS	-0.19	-0.15	-0.16	-0.17		-0.16	-0.17	-0.20	-0.16
Bias	-34.38	-24.42	-26.65	-31.61		-42.14	-34.49	-37.77	-44.91
r	0.23	0.19	0.27	0.23		0.27	0.24	0.23	0.21
CB	0.06	0.12	0.09	0.05		0.02	0.00	0.08	0.04
UCB	0.04	0.03	0.03	0.07		0.17	0.20	0.14	0.12
SS	-0.05	-0.12	-0.05	-0.07		-0.12	-0.15	-0.17	-0.12
Bias	-21.88	-20.35	-20.53	-29.40		-46.43	-50.32	-42.68	-38.53

(a) KF2WJ00

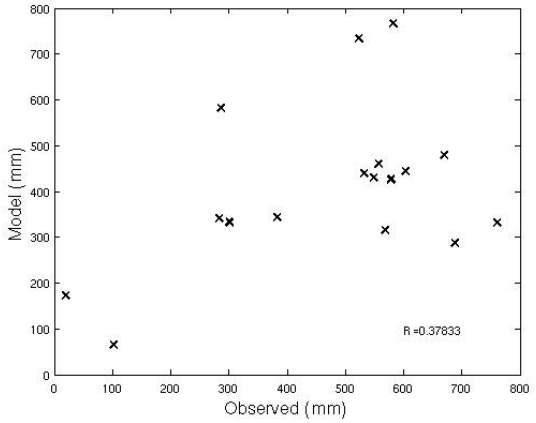

(b) GD2WJ00

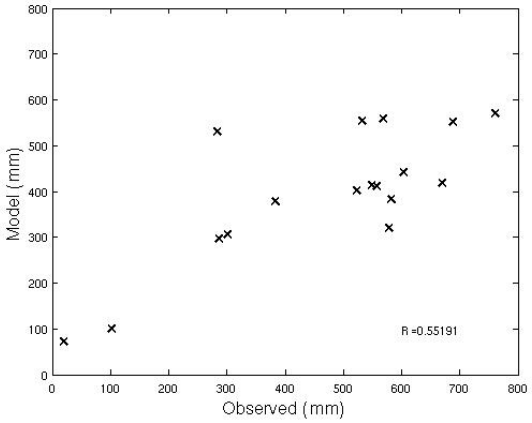

(c) KF1WJ00

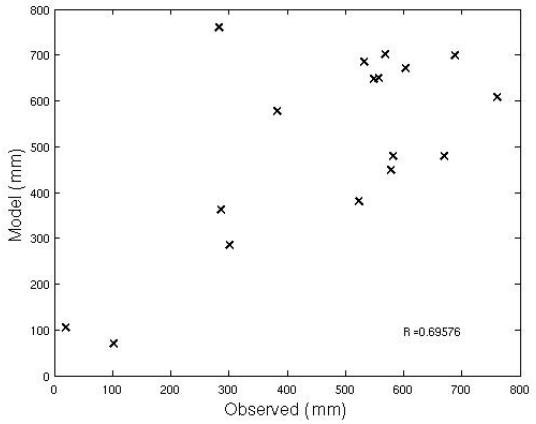

(d) GD1WJ00

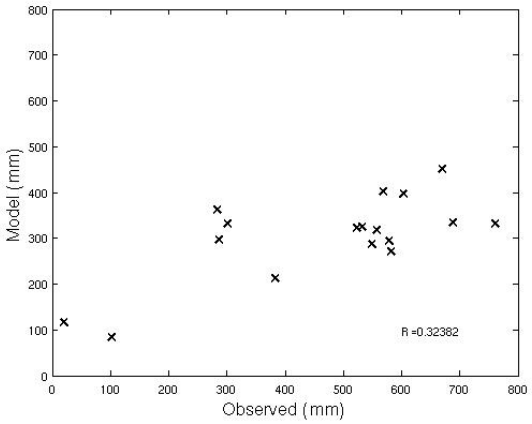

Figure 9. Scatter plots of the monthly precipitation accumulated reported by stations and the monthly precipitation calculated in the nearest grid-points of the inner domain (grids 4). The stations are located in south Caribbean area (blue squares in Fig. 2).

(a) KF2WJ00

(b) GD2WJ00

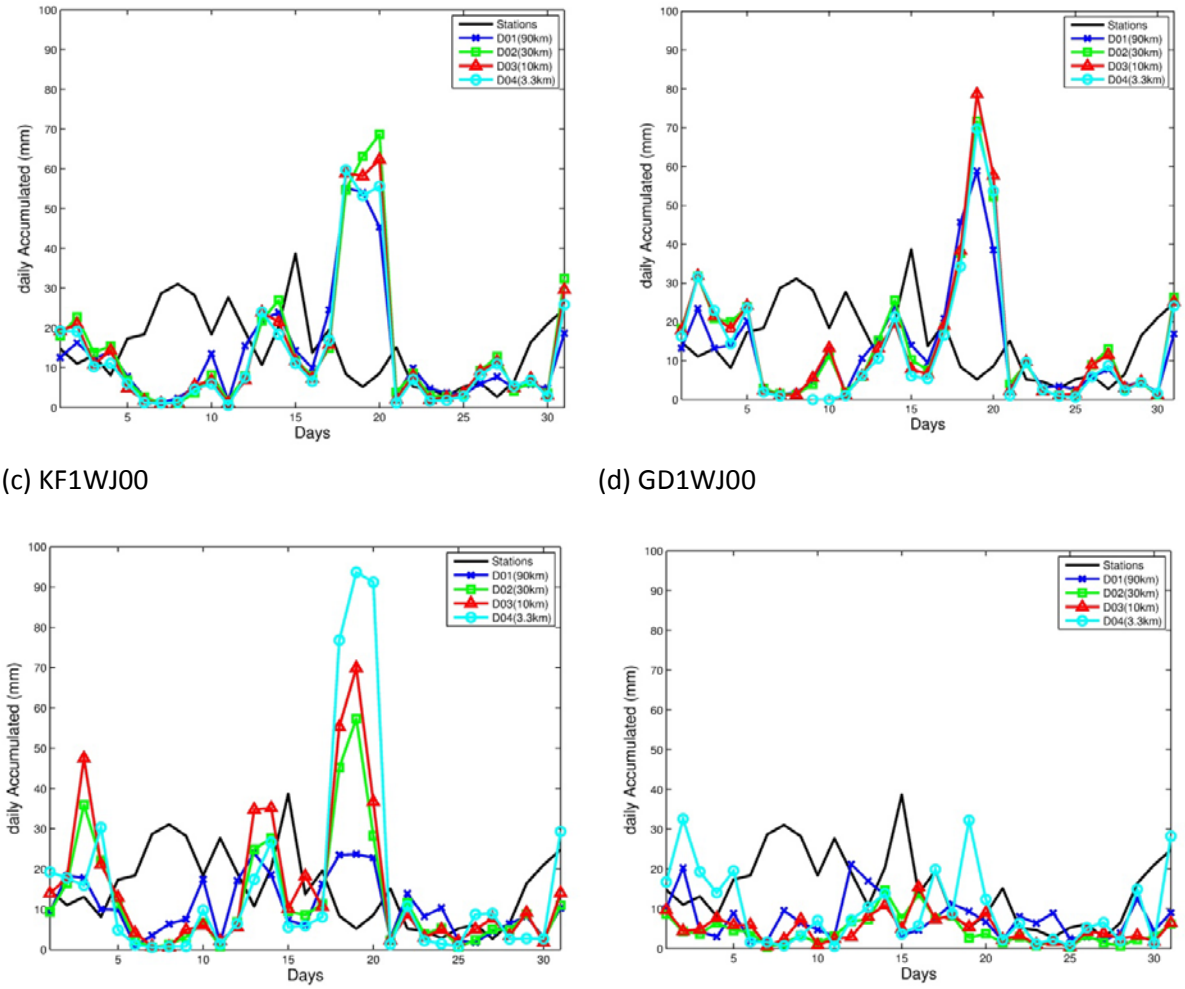

(c) KF1WJ00

(d) GD1WJ00

Figure 10. Time series of stations located in south Caribbean (blue squares, Fig. 2a), and nearest grid-points in each domain during January 2000. The daily precipitation average from all stations located in this area, and from the nearest grid-point to them in domain 4, was calculated to plot the time series.

6.2 September 2007 case

September 2007 experiments showed the same issues (at the boundaries) related to interaction problems discussed above. In grids 1 and 2 (Fig. 11 and 12, respectively), all the experiments revealed an overestimation of rainfall along the ITCZ, furthermore, ITCZ seems to be located further north compared to the experiments for January, which indicates that the model is capturing the annual migration of the ITCZ (also observed in NCEP-NCAR reanalysis, Fig. 3b). Such a surplus is also observed in the inland pattern of rainfall over Central America, being wetter at the Pacific coast during September than in January, as is expected. Both KF2WS07 and KF1WS07 cases show same instabilities close to the Andes. Moreover, all the cases show the area of heavy rainfall nearby the Pacific coast of Colombia, but larger in extension and intensity than during January, in agreement with the annual cycle of average precipitation showed in Poveda and Mesa (2000). Particularly, KF2WS07 (GD1WS07) has the largest (lowest) amount of precipitation in this area.

In domain 3 (Fig. 13), KF1WS07 and GD1WS07 experiments show a particular maximum along the Caribbean coast of Nicaragua that is not found in their corresponding experiments using two-way nesting (KF2WS07 and GD2WS07). Also, these tests produce more precipitation along the Pacific coast of Costa Rica, and Panama, indicating possible intrusions of the ITCZ.

Significant differences on the spatial distribution and amount of precipitation were found in the coarse grids 1, 2 and 3 among the experiments, nonetheless, these discrepancies were not reflected in their corresponding finer domain (Fig. 14), where all the tests show a similar pattern of rainfall upon Central America. However, one could say that those runs allowing one-way nesting tend to produce more precipitation, mainly, along the south boundary, where all seem to capture part of the ITCZ. GD2WS07 and GD1WS07 cases show some intrusions of the ITCZ over southern Pacific coast of Costa Rica. Also, note that 3 of the experiments (KF2WS07, KF1WS07 and GD2S07) detected a relative maximum right over western Caribbean of Panama.

Same precipitation profiles as before were done for experiments S07 (Fig. 15). Larger precipitation spot is located over the Pacific than in the Caribbean side, opposite to January rainfall pattern. KF1WS07 and GD1WS07 tests show a better representation of this pattern in grids 3, not so in domain 4. Other cases do not reproduce this structure. KF2WS07 has the worst results. A KS test (Table 6) indicates that in KF1WS07, GD2WS07, and GD1WS07, domain 3, the null hypothesis is accepted at the 95% of confidence. In agreement with previous results in this study Kain-Fritsch scheme produces more prediction than Grell-Devenyi scheme, feature also found in Mapes et al. (2004). The latter has been associated to the ability of the GD scheme to reproduce spotty but intense rainfall, and apparently is reluctant to activate, frequently yielding little or no rain. However, when rainfall does develop, it is very intense.

Metrics were calculated for the three same areas studied for the January cases, south Caribbean (Table 7), south Pacific (Table 8), and north Central America (Table 9), respectively (Fig. 2b). Note the significant reduction in the number of stations, mainly to the

north, and Caribbean sides. Best results were found in south Caribbean, where 227 mm monthly average was reported by stations. In GD configurations, the inner domain has the highest correlation and skill score. In both cases about the 5% of the monthly precipitation accumulated reported by stations, is overestimated, in disagreement with their respective cases for January. From figure 16, one can see that GD1WS07 has the best fit in a linear regression.

In both south Pacific, and north Central America results exhibit negative and low correlations, and skill score, this suggests that the model is not doing a good performance calculating rainfall over those regions, particularly in south Pacific area, which in turn, also presented the highest amount of the monthly mean precipitation accumulated (535mm).

The time evolution of the model estimations is featureless for September 2007 (not shown). No agreement between observation and prediction was found. So, it gives evidence that using the chosen configuration the model do not reproduce specific events in none case.

(a) KF2WS07

(b) GD2WS07

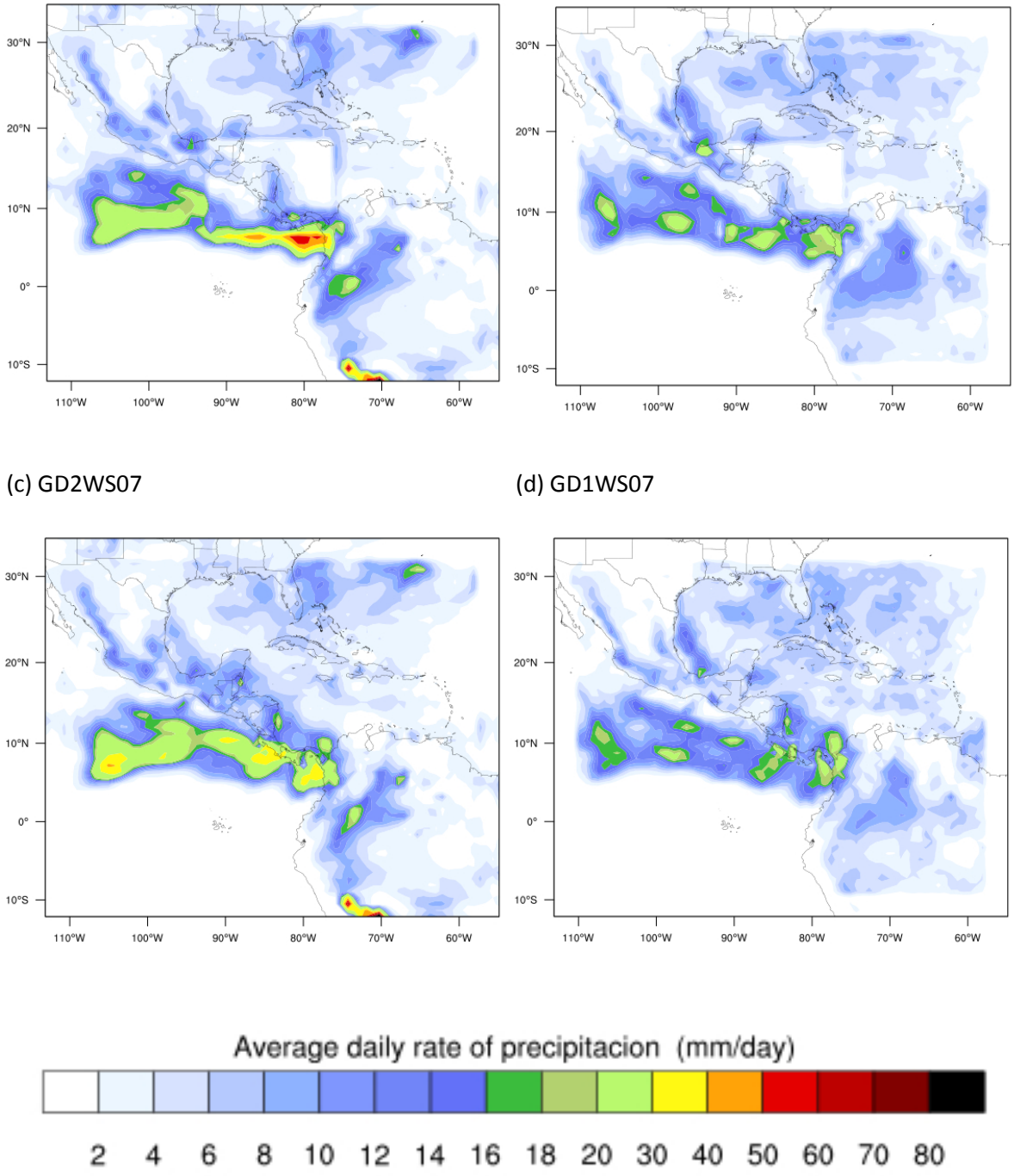

(c) GD2WS07

(d) GD1WS07

Figure 11. Outer grids (90km) in each experiment for September 2007 using (a) and (c) Kain-Fritsch (KF), and (b) and (d) Grell-Devenyi (GD). Also (a) and (b) use two-way nesting; (c) and (d) use one-way nesting for each scheme.

(a) KF2WS07

(b) GD2WS07

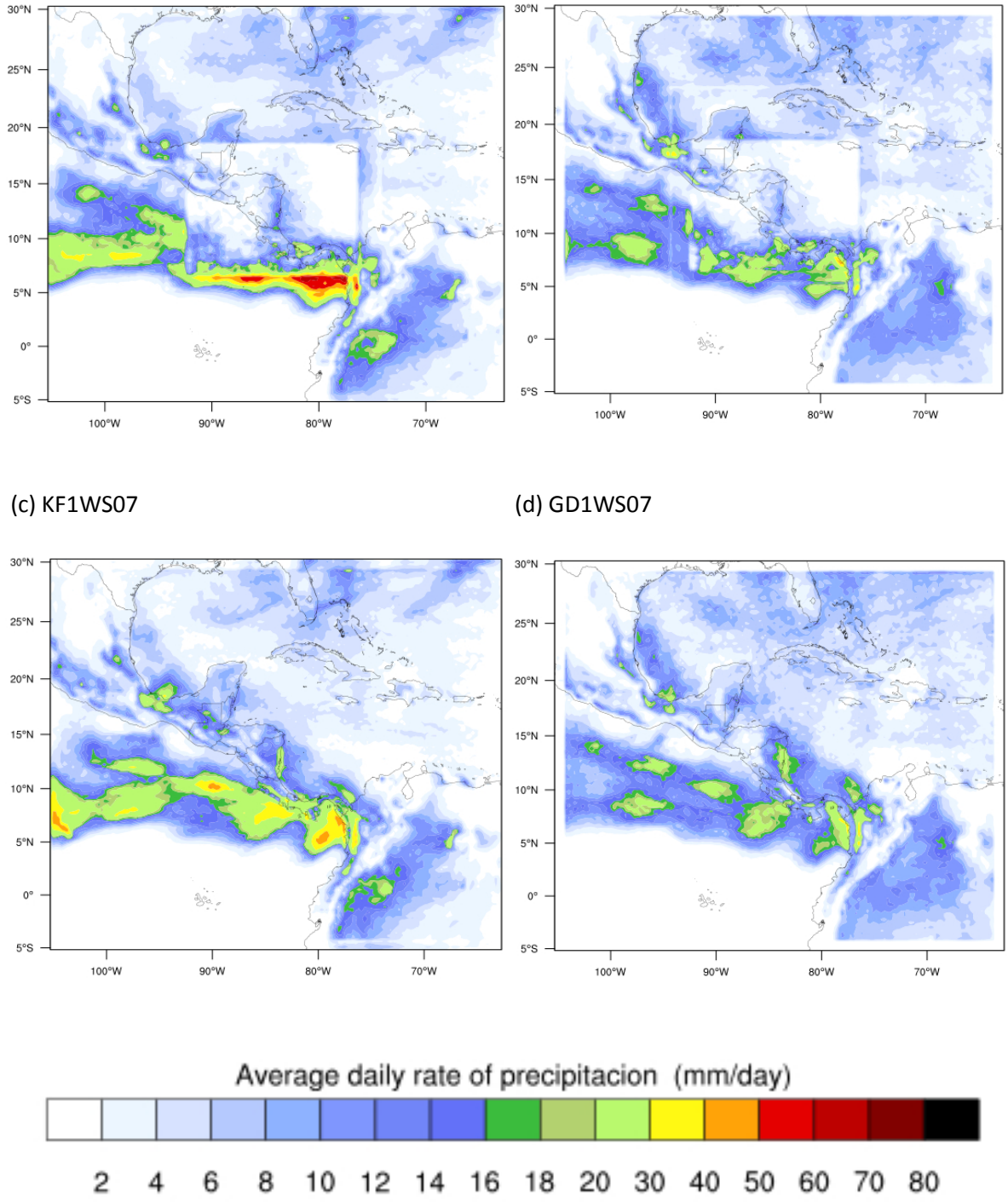

(c) KF1WS07

(d) GD1WS07

Figure 12. As in Fig. 11, but for domain 2 (30km).

(a) KF2WS07

(b) GD2WS07

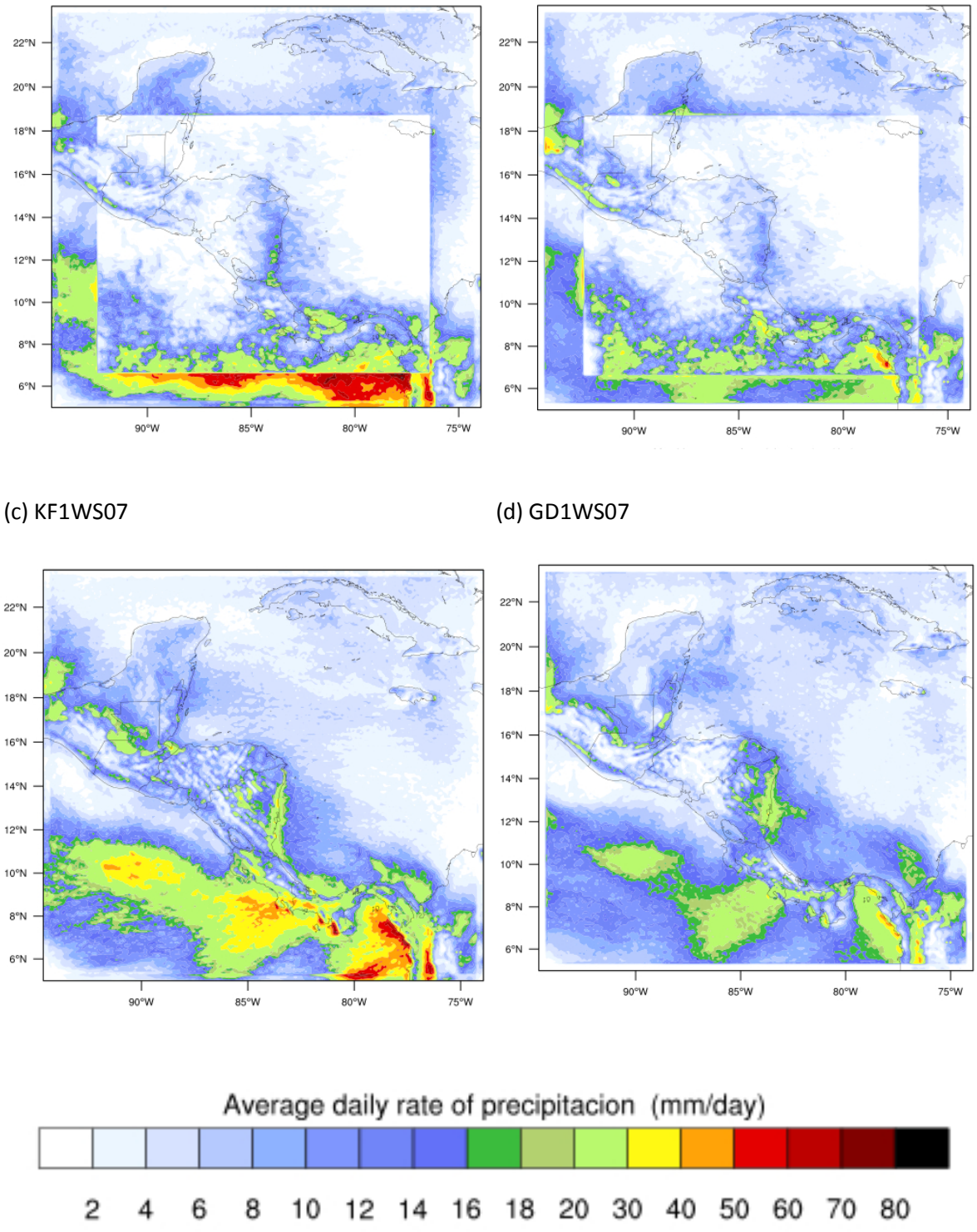

(c) KF1WS07

(d) GD1WS07

Figure 13. As in Fig. 11, but for domain 3 (10km).

(a) KF2WS07

(b) GD2WS07

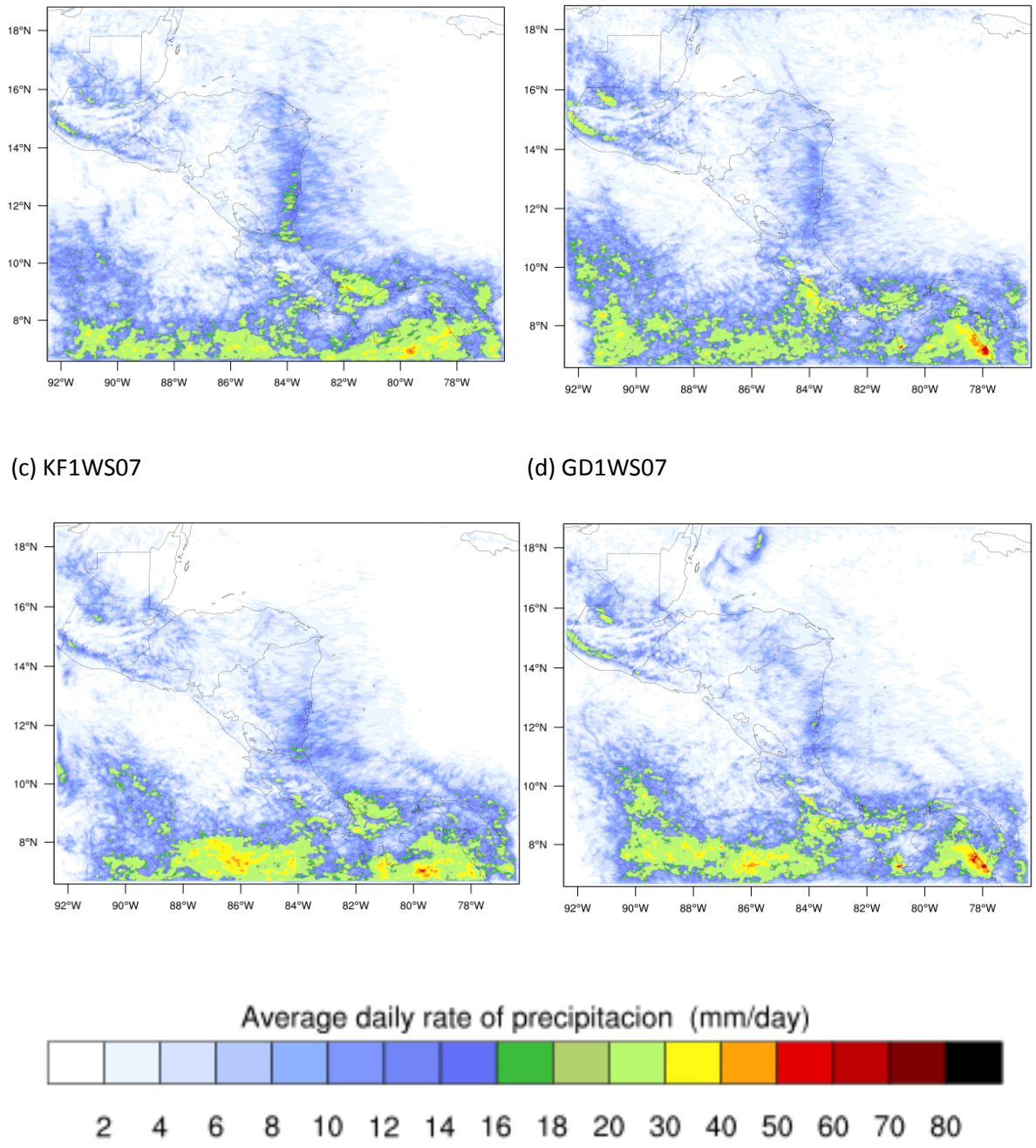

(c) KF1WS07

(d) GD1WS07

Figure 14. As in Fig. 11, but for domain 3 (3.3km).

Table 6. Kolmogorov-Smirnov test for two curves under the hypothesis that both come from the same distribution of data. The test was applied for the monthly precipitation accumulated profiles for September 2007 in Fig. 14. Numbers in bold are within the 95% of confidence level. P-values are in parenthesis.

	(a) KF2WJ00	(b) GD2WJ00	(c) KF1WJ00	(d) GD1J00
D01	0.50(0.01)	**0.33(0.22)**	0.50(0.01)	**039(0.10)**
D02	0.50(0.01)	**0.33(0.22)**	**0.28(0.43)**	**0.22(0.71)**
D03	0.44(0.04)	**0.33(0.22)**	**0.28(0.43)**	**0.22(0.71)**
D04	0.44(0.04)	0.44(0.04)	0.44(0.04)	**0.33(0.22)**

Table 7. Statistical results of each experiment (a) KF2WJ00, (b) GD2WJ00, (c) KF1WJ00 and (d) GD1WJ00. 227mm monthly average accumulated during September 2007 was reported by gauges located in south Caribbean zone (blue squares in Fig. 2b). These stations were compared with the nearest grid-point in each domain. Metrics shown here are the product-moment correlation (r), conditional bias (CB), unconditional bias (UCB), skill score (SS) and bias (B) as in

(a)	d01	d02	d03	d04	(b)	d01	d02	d03	d04
R	0.19	0.26	0.42	0.32		0.24	0.25	0.50	0.48
CB	0.09	0.06	0.04	0.04		0.07	0.10	0.05	0.04
UCB	0.12	0.01	0.04	0.01		0.00	0.00	0.01	0.00
SS	-0.18	-0.01	0.09	0.06		-0.01	-0.04	0.18	0.18
Bias	79.54	27.32	45.12	22.73		14.41	-3.82	27.32	11.02
(c)					(d)				
R	-0.05	0.46	0.48	0.31		0.22	0.42	0.90	0.85
CB	0.28	0.28	0.04	0.02		0.16	0.31	0.01	0.13
UCB	0.99	0.12	0.30	0.00		0.20	0.00	0.01	0.00
SS	-1.39	-0.21	-0.15	0.07		-0.34	-0.13	0.79	0.59
Bias	231.15	81.97	128.42	11.73		103.51	-10.39	21.62	16.08

Table 8. As in Table 3 but for the south Pacific (black squares in Fig 2b), and 535mm monthly average accumulated was reported by the stations.

(a)	d01	d02	d03	d04	(b)	d01	d02	d03	d04
R	-0.20	-0.05	0.01	-0.01		-0.16	0.05	0.01	0.00
CB	0.13	0.10	0.10	0.11		0.13	0.07	0.10	0.09
UCB	0.21	0.22	0.21	0.23		0.13	0.13	0.16	0.19
SS	-0.31	-0.33	-0.32	-0.35		-0.24	-0.20	-0.26	-0.28
Bias	-285.36	-291.10	-284.17	-297.33		-223.53	-222.97	-248.01	-269.08
(c)					(d)				
R	0.04	0.26	0.16	0.08		-0.08	-0.11	0.28	0.02
CB	0.06	0.00	0.03	0.02		0.05	0.06	0.00	0.09
UCB	0.00	0.04	0.00	0.26		0.07	0.12	0.06	0.17
SS	-0.06	0.02	-0.01	-0.28		-0.12	-0.17	0.02	-0.28
Bias	34.07	-126.81	31.90	-314.95		-166.62	-211.86	-148.89	-260.09

Table 9. As in Table 3 but for the north Central America (green squares in Fig 2b), and 116mm monthly average accumulated was reported by the stations.

(a)	d01	d02	d03	d04	(b)	d01	d02	d03	d04
R	0.10	0.03	0.00	0.05		-0.04	-0.13	-0.16	-0.12
CB	0.13	0.60	0.93	0.80		0.37	1.44	1.58	1.43
UCB	0.01	0.07	0.02	0.02		0.05	0.29	0.12	0.11
SS	-0.13	-0.66	-0.95	-0.82		-0.42	-1.73	-1.68	-1.54
Bias	10.23	33.13	18.21	18.09		28.05	69.59	43.92	42.61
(c)					(d)				
R	0.47	0.23	0.72	-0.01		0.58	0.09	0.47	-0.23
CB	0.12	0.64	1.85	0.70		0.07	0.56	0.31	1.76
UCB	0.99	1.70	3.54	0.00		0.13	0.27	0.35	0.06
SS	-0.95	-2.39	-5.05	-0.70		0.12	-0.84	-0.47	-1.77
Bias	128.66	168.49	243.19	-0.75		46.92	67.07	76.88	31.41

(a) KF2WS07

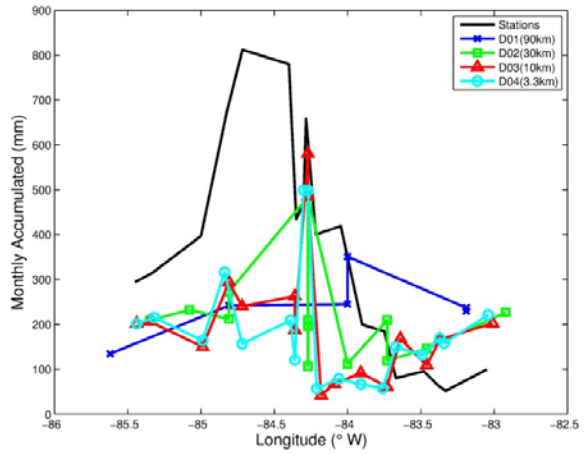

(b) GD2WS07

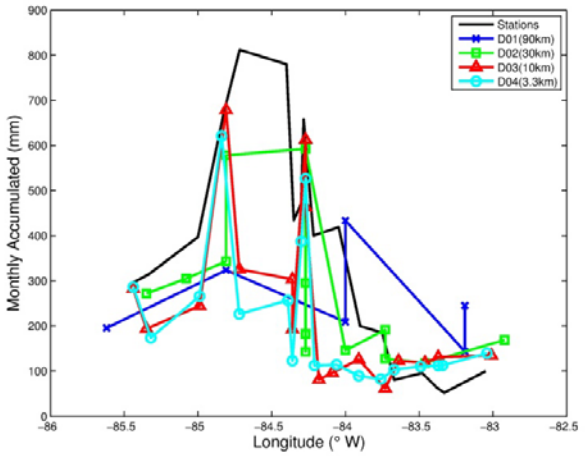

(c) KF1WS07

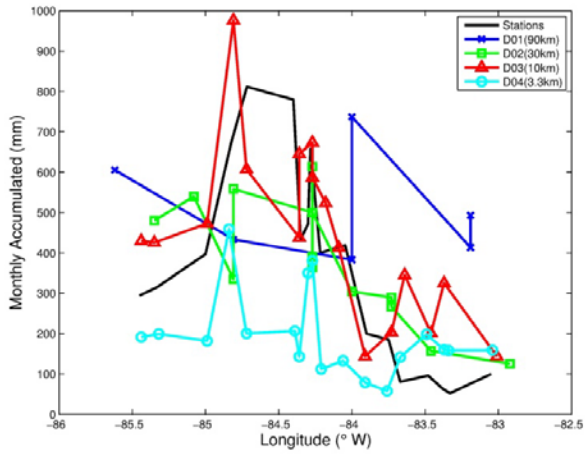

(d) GD1WS07

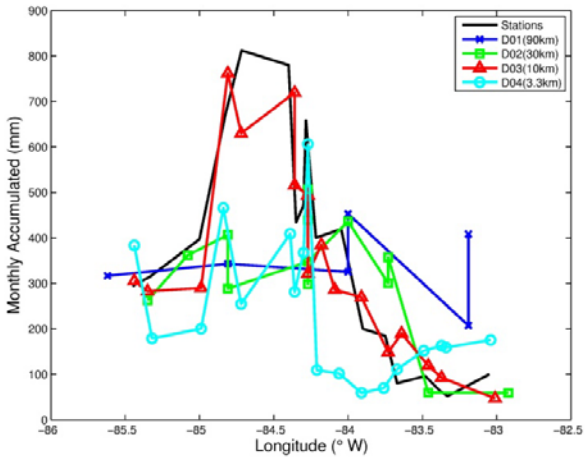

Figure 15. As in Fig. 8, but for September 2007.

(a) KF2WS07

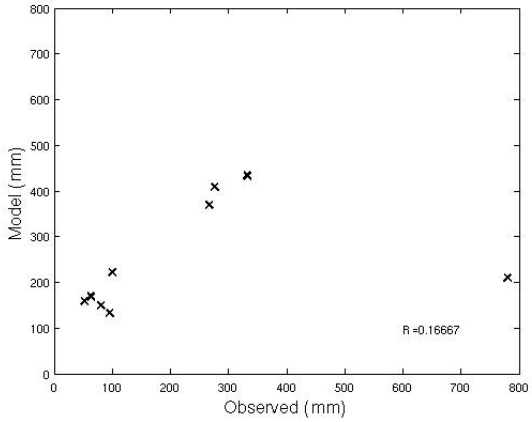

(b) GD2WS07

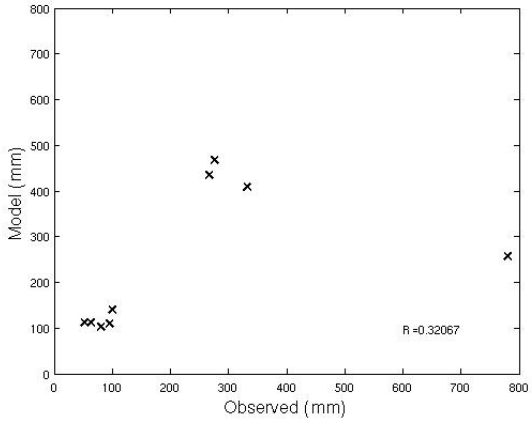

(c) KF1WS07

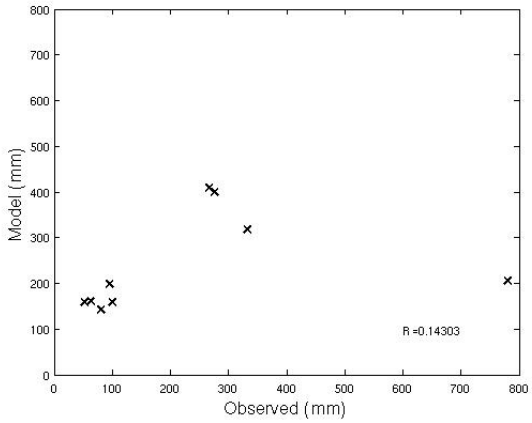

(d) GD1WS07

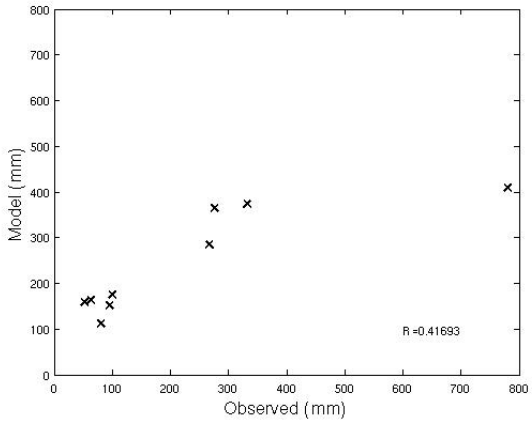

Figure 16. As in Fig. 9, but for September 2007.

7. Discussion

Statistics of the inner grids indicated that GD2WJ00 and KF1WJ00 tests have the highest correlation and skill score over the high precipitation region (Table 3), but being underestimated and overestimated, respectively. The other two cases shown a negative skill score, and in G1WJ00 precipitation was underestimated about twice compared to the others. In south Pacific (Table 4), statistics also showed good results, but rainfall was underestimated in all the experiments. This region and north Central America (Table 5), low precipitation events were observed and estimated, hence, these results should be taken carefully. In the latter region, statistics showed low correlations and negative skill score in all the cases.

The outputs from September 2007 experiment showed two interesting results. First, despite some variances were found among the different cases in the coarse resolution domains (1, 2, and 3, Fig. 11, 12 and 13, respectively), in which implicit and explicit convection schemes were used, however, the inner grids (Fig. 14) seemed to not be affected by that forcing, mainly in one-way nesting experiments. Second, notice that in south Central America, more rainfall was observed by stations in the Pacific than the Caribbean side. This pattern was not detected as good as in the January case by the model (Fig. 15), barely detected in the grids 3 (10km) in KF1WS00 and GD1WS00 tests.

In south Caribbean stations, the largest correlation, and skill score were found in GD1WS00 case. The lowest skill was found in KF experiments. Furthermore, in domain 4, all the cases overestimated the amount in about the order of 15mm, which represents the 7% of the monthly average accumulated reported by stations upon this region. However, in south Pacific (Table 7) and north Central America (Table 8), those statistics indicate a pessimist performance due to the low correlations and negative skill score that were found in inner domain.

In south Pacific region the metrics indicate that the model do not reproduce heavy precipitation events, since precipitation is highly underestimated compared to the amount reported by stations during September 2007.

In north Central America, neither January 2000 nor September 2007 cases did not show high correlation and skill score. Notice, however, that during the first month precipitation was underestimated, whereas in the second month, it was overestimated.

The poor performance showed in September 2007 experiments, compared to the observations, could be associated to that during September 2007 a transition to a cold El Niño episode (La Niña) was observed. However, the boundary conditions used, the NCEP/NCAR Reanalysis data, have showed difficulty in representing transitions from weak warm to cold ENSO episodes (Janowiak et al. 1998). Those deficiencies, thus, could be affecting the results in the mesoscale model.

Moreover, in general, experiments using Kain-Fritsch scheme calculated more precipitation than experiments using Grell-Devenyi scheme. Similar result was found in (Mapes et al. 2004), and Rivera and Amador (2009). The latter has been associated with the

activation of the GD scheme, because it is hesitant to activate, but when rain develops, it is very intense and irregular.

Despite that climatically the model outputs are acute mainly in the Caribbean side, during January; time series of all the experiments, do not replicate specific precipitation events, and thus, the 5-days configuration is not enough to reproduce short-period events.

Moreover, same irregular patterns in the precipitation field found in Warner and Hsu (2000), and Bukovsky and Karoly (2009), were also observed in this study. These irregularities reveal some physical problems that are still present in the current cumulus parameterization schemes, since they coincide with the region where the inner domain is defined within the domains 1, 2 and 3. It should be noted that this pattern appears only when two-way nesting was allowed. In addition, such discontinuities were observed both in the daily average precipitation rates field, and also in lower frequency rates, like in the 6 hours rainfall accumulated (not shown here). In spite of so, the estimated precipitation in the inner grids is not affected; hence, this annotation should be taking into account at the moment of defining the domain configuration, and the integration time for future simulations.

8. Summary and Conclusions

Precipitation was estimated employing dynamical downscaling techniques for January 2000 and September 2007 using the regional climate model WRF, and the NCEP-NCAR Reanalysis Project (Kalnay et al. 1996, Kistler et al. 2001) data as boundary and initial conditions. Four-nested-domains were configured (Fig. 1a) over Central America. The runs were reinitialized each 5 days with 6 hours spin-up time for adjustment of the model. Two cumulus convection schemes, Kain-Fritsch (Kain 2004) and Grell-Devenyi (Grell and Dévényi 2002), were tested for each month simulated. Besides that, the physical interaction among nested domains was examined. First, the model was allowed to have feedback among nested domains (two-way nesting), and second, the model makes calculation just in one direction, from the outer to the inner domain (one-way nesting). For comparison, daily precipitation data from gauge stations were divided in three important regions (Fig. 2) according to local precipitation structures observed, and to the quality of the data reported by the stations during each month.

January 2000 results showed that the model is detecting mean climate features on magnitude, and spatial distribution during this month, either in mesoscale resolution grids (1 and 2, Fig. 4 and 5), or finer resolution domains (3 and 4, Fig. 6 and 7). Important to note the contrast in the precipitation structure over southern Central America observed by the stations and in model outputs, having a maximum upon south Caribbean region (Fig. 8). This is in agreement with the climatology during this season reported by Alfaro (2002), Taylor and Alfaro (2005), Amador et al. (2006). In addition, this result reflects the ability of the model to solve the interaction between the topography and the northeasterly flow during January in this region.

Results showed that WRF model has some ability in reproducing the main precipitation structures (on spatial distribution and magnitude), that were also noted in the observed data, and in agreement also with the climatology, mainly during January 2000. While, results from September 2007 experiments, disagreed substantially with observations, and climatology. Despite that, results suggest that this kind of technique (dynamical downscaling) could be used to study the climatology of regional and local scale circulations as the IALLJ or the Chocó jet, which are very important elements in producing rainfall in Central America, since results showed that this model is also capable to capture the interaction between sharp topography and the easterly wind flow.

Furthermore, notice that the poor performance during September 2007 experiments can be related with some issues found in the boundary conditions (NCEP/NCAR data), such as this GCM has difficulty in reproduce transitions from warm to cold ENSO episodes (Janowiak et al. 1998). In addition, these authors also found that the reanalysis data have a good representation of main climate features of precipitation at global scale, however, at regional and local scales this model fails, due mainly to a poor representation of sharp topography gradients, like the Andes or high mountains in Central America. Besides that, this GCM has showed some deficiencies to capture seasonal variability, and the seasonal migration of the ITCZ, and hence, difficulty in representing major climate features in tropical regions. Given that, further examination of the influence of the boundaries conditions in the regional models over this region is suggested, and why not to use other reanalysis data as boundary conditions such as the ERA-Interim reanalysis model (Dee et al. 2011) or the GFS analysis model (Whitaker et al. 2008).

Moreover, the integration period, including the spin-up time (5 days plus 6 hours), used for simulations in this study, is not adequate to represent specific events, but did a good estimation of the daily precipitation rates, climatologically speaking. However, it should be noticed that during either January or September, meso- and small scale events such as cold surges during the first month, or the “temporales” in the second case, are very important mechanism in producing rainfall in the isthmus. The latter is opening the doors to explore other integration periods, possibly shorter than the used here, in order to study such kind of events.

In experiments using two-ways nesting, discontinuities in precipitation fields were found in domains 1, 2 and 3, which all used a hybrid convection scheme (explicit and implicit). Such discontinuities coincide with the same area, where the inner domain is defined, and which only explicit convection scheme is used. Such irregular patterns were not observed in other variables like temperature, wind or humidity field (not shown). Similar irregular patterns were firstly reported by Warner and Hsu (2000) using MM5 model, and, then, by Bukovsky and Karoly (2009) using WRF model. Therefore, that result provides evidence that there still are problems in the current cumulus schemes in mesoscale models, which are not model dependent. Such issues, nevertheless, have been related to the adjustment of the mass field between the inner and outer domains (Warner and Hsu 2000), but also with the formulation of the cumulus convection problem itself (Arakawa 2004).

Acknowledgements

I would like to thank to my supervisors Anna Rutgersson, Jorge A. Amador, and Eric J. Alfaro, for their comments, guidance, patience, and support to my work. Also, thanks to the International Science Program for funding my studies at Uppsala University, and, finally, but not less, to my mother, and my friends, they always be when I need them.

References

Alcántara-Ayala, I., 2002: Geomorphology, natural hazards, vulnerability and prevention of natural disasters in developing countries. *Geomorphology*, **47**, 107–124.

Alfaro, E., 2000: Eventos cálidos y fríos en el Atlántico tropical norte. *Atmosfera*, **13**, 109–119.

Alfaro, E., 2002: Some Characteristics of the Annual Precipitation Cycle in Central America and their Relationships with its Surrounding Tropical Oceans. *Tópicos Meteorológicos y Oceanográficos*, **9**, 1–13.

Alfaro, E., 2007: Uso del análisis de correlación canónica para la predicción de la precipitación pluvial en Centroamérica. *Revista Ingeniería y Competitividad*, **9**, 33-48.

Alfaro, E., and L. Cid, 1999a: Ajuste de un modelo VARMA para los campos de anomalías de precipitación en Centroamérica y los índices de los océanos Pacífico y Atlántico tropical. *Atmosfera*, **12**, 205-222.

Alfaro, E., and L. Cid, 1999b: Análisis de las anomalías en el inicio y el término de la estación lluviosa en Centroamérica y su relación con los océanos Pacífico y Atlántico tropical. *Tópicos Meteorológicos Oceanográficos*, **6**, 1-13.

Alfaro, E., L. Cid, and D. Enfield, 1998: Relaciones entre la precipitación en Centroamérica y los Océanos Pacífico y Atlántico Tropical. *Investigaciones Marinas*, **26**, 59-69.

Alfaro, E., A. Quesada, and F. Solano, 2010: Análisis del impacto en Costa Rica de los ciclones tropicales ocurridos en el Mar Caribe desde 1968 al 2007. *Revista Diálogos*, **11**, 22–38.

Amador, J. A., 1998: A climate feature of the tropical Americas: the trade wind easterly jet. *Tópicos Meteorológicos y Oceanográficos*, **5**, 91-102.

Amador, J. A., 2008: The Intra-Americas Sea Low-level Jet. *Ann. N. Y. Acad. Sci.*, **1146**, 153-188.

Amador, J. A., and E. Alfaro, 2009: Métodos de reducción de escala: aplicaciones al tiempo, clima, variabilidad climática y cambio climático. *Revista Iberoamericana de Economía Ecológica*, **11**, 39–52.

Amador, J. A., and V. O. Magaña, 1999: Dynamics of the low-level jet over the Caribbean Sea. Preprints, *23rd Conf. on Hurricanes and Tropical Meteorology, Dallas*, TX, Amer. Meteor. Soc., 868-869.

Amador, J. A., V. O. Magaña, and J. B. Pérez, 2000: The low-level jet and convective activity in the Caribbean. Preprints, *24th Conf. on Hurricanes and Tropical Meteorology, Fort Lauderdale*, FL, Amer. Meteor. Soc., 114-115.

Amador, J. A., R. E., Chacón, and S. Laporte, 2003: Climate and climate variability in the Arenal Basin of Costa Rica. Climate and Water: *Transboundary Challenges in the Americas*. H. F., Morehouse, B., Ed., Klewer Academic Publishers BV, 317-350.

Amador, J. A., E. J. Alfaro, O. G. Lizano, and V. O. Magaña, 2006: Atmospheric forcing of the eastern tropical Pacific: A review. *Prog. Oceanogr.*, **69**, 101–142.

Arakawa, A., 2004: The Cumulus Parameterization Problem: Past, Present, and Future. *J. Climate*, **17**, 2493–2525, doi:10.1175/1520-0442(2004)017<2493:RATCPP>2.0.CO;2.

Banichevich, A., and O. G. Lizano, 1998: Interconexión a nivel ciclónico-atmosférico entre el Caribe y el Pacífico. *Rev. Biol. Trop.*, **46**, 9-21.

Bukovsky, M. S., and D. J. Karoly, 2009: Precipitation Simulations Using WRF as a Nested Regional Climate Model. *J. Appl. Meteor. Climatol.*, **48**, 2152–2159.

Cronin, M. F., N. Bond, C. Fairall, J. Hare, M. J. McPhaden, and R. A. Weller, 2002: Enhanced oceanic and atmospheric monitoring underway in the eastern Pacific. *EOS, Trans. Amer. Geophys. Union*, **83**, 210-211.

da Silva, A. M., and S. Levitus, 1994: *Anomalies of Heat and Momentum Fluxes.* Vol. 3*, Atlas of Surface Marine Data 1994*, U.S. Department Commerce, 413 pp.

Davis, C., and Coauthors, 2008: Prediction of Landfalling Hurricanes with the Advanced Hurricane WRF Model. *Mon. Wea. Rev.*, **136**, 1990–2005.

Dee, D. P., and Coauthors, 2011: The ERA-Interim reanalysis: configuration and performance of the data assimilation system. *Q. J. R. Meteorol. Soc.*, **137**, 553-597.

Donoso, M., and Ramírez, P., 2001: Latin America and the Caribbean: Report on the Climate Outlook Forums for Mesoamerica. In: Coping with the climate: A step Forward. Workshop Report: A multi-stakeholder review of Regional Climate Outlook Forums, Pretoria, South Africa, 16–20 October 2000, Publication IRI-CW/01/1, 11-18, 2001.

Dudhia, J., 1989: Numerical Study of Convection Observed during the Winter Monsoon Experiment Using a Mesoscale Two-Dimensional Model. *J. Atmos. Sci*., **46**, 3077–3107.

Dudhia, J., D. Gill, Y.-R. Guo, K. Manning, W. Wang, and C. Bruyere, cited 2012: PSU/NCAR Mesoscale Modeling System Tutorial Class Notes and User's Guide: MM5 Modeling System Version 3.

Dudhia, J., S-Y. Hong, and K-S. Lim, 2008: A new method for representing mixed-phase particle fall speeds in bulk microphysics parameterizations. *J. Meteor. Soc. Japan*, **86A**, 33-44.

Enfield, D. B., and E. J. Alfaro, 1999: The Dependence of Caribbean Rainfall on the Interaction of the Tropical Atlantic and Pacific Oceans. *J. Climate*, **12**, 2093–2103.

Enfield, D.B., S.-K. Lee, and C. Wang, 2006: How are large western hemisphere warm pools formed?, *Prog. Oceanogr.*, **70,** 346-365.

Garcia-Solera, I., and P. Ramirez, 2012: Central America's Seasonal Climate Outlook Forum. The Climate Services Partnership, 8pp. Available at http://climate-services.org/resource/central-american-climate-outlook-forum

Gershunov, A., T. P. Barnett, D. R. Cayan, T. Tubbs, and L. Goddard, 2000: Predicting and Downscaling ENSO Impacts on Intraseasonal Precipitation Statistics in California: The 1997/98 Event. *J. Hydrometeor.*, **1**, 201–210.

Giorgi, F., and L. O. Mearns, 1999: Introduction to special section: Regional climate modeling revisited. *J. Geophys. Res.*, **104**, 6335–6352.

Gochis, D. J., W. J. Shuttleworth, and Z.-L. Yang, 2002: Sensitivity of the Modeled North American Monsoon Regional Climate to Convective Parameterization. *Mon. Wea. Rev.*, **130**, 1282–1298.

Goldenberg, S., C. Landsea, A. Mestas-Nuñez, and W. Gray, 2001: The increase in Atlantic hurricane activity: Causes and Implications. *Science*, **293**, 474-479.

Grell, G., and D. Devenyi, 2002: A generalized approach to parameterizing convection combining ensemble and data assimilation techniques. *Geophys. Res. Lett.*, **29**, 1693.

Grell, G. A., J. Dudhia, and D. R. Stauffer, 1994: A description of the fifth generation Penn State/NCAR mesoscale model. NCAR, Boulder, Colorado, USA.

Hanstenrath, S., 1991: *Climate Dynamics of the Tropics*. Kluwer Academic Publishers, 488 pp.

Hernandez, J. L., J. Srikishen, D. J. Erickson III, R. Oglesby, and D. Irwin, 2006: A regional climate study of Central America using the MM5 modeling system: results and comparison to observations. *International Journal of Climatology*, **26**, 2161–2179.

Holton, J. R., 2004: *An Introduction to Dynamic Meteorology*. Academic Press Inc, 535 pp.

Hong, S.-Y., and H.-L. Pan, 1996: Nonlocal Boundary Layer Vertical Diffusion in a Medium-Range Forecast Model. *Mon. Wea. Rev.*, **124**, 2322–2339.

Instituto Meteorológico Nacional, 2000: Boletín Meteorológico Mensual – Enero 2000, 19 pp.

Instituto Meteorológico Nacional, 2007: Boletín Meteorológico Mensual – Septiembre 2007, 21 pp.

Janowiak, John E., Arnold Gruber, C. R. Kondragunta, Robert E. Livezey, George J. Huffman, 1998: A Comparison of the NCEP-NCAR Reanalysis Precipitation and the GPCP Rain Gauge-Satellite Combined Dataset with Observational Error Considerations. *J. Climate*, **11**, 2960-2979.

Kain, J. S., 2004: The Kain–Fritsch Convective Parameterization: An Update. *J. Appl. Meteor.*, **43**, 170–181.

Kain, J. S., and J. M. Fritsch, 1990: A One-Dimensional Entraining/Detraining Plume Model and Its Application in Convective Parameterization. *J. Atmos. Sci.*, **47**, 2784–2802.

Kain, J. S., and J. M. Fritsch, 1992: The role of the convective ”trigger function” in numerical forecasts of mesoscale convective systems. *Meteor. Atmos. Phys.*, **49**, 93–106.

Kalnay, E., and Coauthors, 1996: The NCEP/NCAR 40-Year Reanalysis Project. *Bull. Amer. Meteor. Soc.*, **77**, 437-471.

Kistler, R. and Coauthors, 2001: The NCEP–NCAR 50–Year Reanalysis: Monthly Means CD–ROM and Documentation. *Bull. Amer. Meteor. Soc.*, **82**, 247–267.

Lawrimore, Jay H., and Coauthors, 2001: Climate Assessment for 2000. *Bull. Amer. Meteor. Soc.*, **82**, 1304-1304.

Lee, S.-K., D.B. Enfield, and C. Wang, 2007: What drives the seasonal onset and decay of the western hemisphere warm pool?, *J. Climate*, **20,** 2133-2146.

Levinson, D. H., J. H. Lawrimore, 2008: State of the Climate in 2007. *Bull. Amer. Meteor. Soc.*, **89**, S1-S179.

Louis, J. F., 1979: A parametric model of vertical eddy fluxes in the atmosphere. *Bound.-Layer Meteor.*, **17**, 187-202.

Magaña, V., J. A. Amador, and S. Medina, 1999: The Midsummer Drought over Mexico and Central America. *J. Climate*, **12**, 1577–1588.

Maldonado, T., and E. Alfaro, 2010a: Comparación de las salidas del modelo MM5v3 con datos observados en la Isla del Coco, Costa Rica. *Tecnología en Marcha*, **23**, 3–28.

Maldonado, T. and E. Alfaro, 2010b: Propuesta metodológica para la predicción climática estacional de eventos extremos y días con precipitación. Estudio de caso: Sur de América Central. *Revista Intersedes*, **11**, 182-214.

Maldonado, T. and E. Alfaro, 2011: Predicción estacional para ASO de eventos extremos y días con precipitación sobre las vertientes Pacífico y Caribe de América Central, utilizando análisis de correlación canónica. *Revista Intersedes*, **12**, 78-108.

Manuel-Navarrete, D., J. J. Gómez, and G. Gallopín, 2007: Syndromes of sustainability of development for assessing the vulnerability of coupled human–environmental systems. The case of hydrometeorological disasters in Central America and the Caribbean. *Global Environmental Change*, **17**, 207–217.

Mapes, B. E., T. T. Warner, M. Xu, and D. J. Gochis, 2004: Comparison of Cumulus Parameterizations and Entrainment Using Domain-Mean Wind Divergence in a Regional Model. *J. Atmos. Sci.*, **61**, 1284–1295.

Mass, C. F., D. Ovens, K. Westrick, and B. A. Colle, 2002: Does Increasing Horizontal Resolution Produce More Skillful Forecasts?, *Bull. Amer. Meteor. Soc.*, **83**, 407–430.

Molinari, J., and M. Dudek, 1992: Parameterization of Convective Precipitation in Mesoscale Numerical Models: A Critical Review. *Mon. Wea. Rev.*, **120**, 326–344.

Morales Méndez, J. F., 2010: Comparison of two rainfall - runoff models in catchment with limited rainfall data - Samalá River, Guatemala. Uppsala University, 55 pp.

Pan, H.-L., and W.-S. Wu, 1994: Implementing a mass flux convection parameterization package for the NMC medium-range forecast model. Preprints, *Vol. 96-98 of, 10th Conference on Numerical Weather Prediction, Portland*, OR, Amer. Meteor. Soc.,
40 pp.

Pierce, D. W., T. P. Barnett, B. D. Santer, and P. J. Gleckler, 2009: Selecting global climate models for regional climate change studies. *Proceedings of the National Academy of Sciences*, **106**, 8441 –8446.

Pleim, J. E., and A. Xiu, 1995: Development and Testing of a Surface Flux and Planetary Boundary Layer Model for Application in Mesoscale Models. *J. Appl. Meteor.*, **34**, 16–32.

Poveda, G., and O. J. Mesa, 2000: On the existence of Lloró (the rainiest locality on Earth): Enhanced ocean-land-atmosphere interaction by a low-level jet. *Geophys. Res. Lett.*, **27**, 1675–1678.

Qian, J.-H., A. Seth, and S. Zebiak, 2003: Reinitialized versus Continuous Simulations for Regional Climate Downscaling. *Mon. Wea. Rev.*, **131**, 2857–2874.

Quesada Montano, B., 2011: Historical Daily Precipitation Patterns for Central America Generated Using Constructed Analogues from Satellite and Ground-Based Observations. Uppsala University, 18 pp.

Ray, P., C. Zhang, M. Moncrieff, J. Dudhia, J. Caron, L. Ruby Leung, and C. Bruyere, 2011: Role of the atmospheric mean state on the initiation of the Madden-Julian oscillation in a tropical channel model. *Climate Dynamics*, **36**, 161–184.

Reynolds, E., 2012: Usability of Standard Monitored Rainfall-Runoff Data in Panama, Juan Diaz River. Uppsala University, 62 pp.

Rivera, E. R., and J. A. Amador, 2009: Predicción estacional del clima en Centroamérica mediante la reducción de escala dinámica. Parte II: aplicación del modelo MM5V3. *Revista de Matemática: Teoría y Aplicaciones*, **16**, 76–104.

Schultz, D. M., W. E. Bracken, L. F. Bosart, G. J. Hakim, M. A. Bedrick, M. J. Dickinson, and K. R. Tyle, 1997: The 1993 Superstorm Cold Surge: Frontal Structure, Gap Flow, and Tropical Impact. *Mon. Wea. Rev.*, **125**, 5–39.

Schultz, D. M., W. E. Bracken, and L. F. Bosart, 1998: Planetary- and Synoptic-Scale Signatures Associated with Central American Cold Surges. *Mon. Wea. Rev.*, **126**, 5–27.

Skamarock, W. C., J. B. Klemp, J. Dudhia, D. O. Gill, D. M. Barker, W. Wang, and J. G. Powers, 2008: A description of the Advanced Research WRF version 3. NCAR Tech. Note NCAR/TN-475+STR, 113 pp.

Stensrud, D. J., R. L. Gall, S. L. Mullen, and K. W. Howard, 1995: Model Climatology of the Mexican Monsoon. *J. Climate*, **8**, 1775–1794.

Srinivasan, J., G. L. Smith, 1996: Meridional Migration of Tropical Convergence Zones. *J. Appl. Meteor.*, **35**, 1189-1202.

Taylor, M. A., and E. J. Alfaro, 2005: Climate of Central America and the Caribbean. *Encyclopedia of World Climatology*, J.E. Oliver, Ed., Springer, 183–186.

Trenberth, K. E., 2010: *Climate System Modeling*. Cambridge University Press, 822 pp.

Vaidya, S. S., 2007: Simulation of weather systems over Indian region using mesoscale models. *Meteor. Atmos. Phys.*, **95**, 15–26.

Velásquez, R.C., 2000: Mecanismos físicos de variabilidad climática y eventos extremos en Venezuela. Tesis de Licenciatura en Meteorología, Departamento de Física Atmosférica, Oceánica y Planetaria, Escuela de Física, Universidad de Costa Rica, 118pp. (Available at Biblioteca Central, Universidad de Costa Rica, 2060 San José, Costa Rica).

Wang, C., and D. B. Enfield, 2001: The Tropical Western Hemisphere Warm Pool. *Geophys. Res. Lett.*, **28**, 1635–1638.

Wang, C., and D. B. Enfield, 2003: A Further Study of the Tropical Western Hemisphere Warm Pool. *J. Climate*, **16**, 1476–1493.

Wang, C., and P. Fielder, 2006: ENSO variability in the eastern tropical Pacific: A review. *Prog. Oceanogr.*, **69**, 239-266.

Wang, W., and N. L. Seaman, 1997: A Comparison Study of Convective Parameterization Schemes in a Mesoscale Model. *Mon. Wea. Rev.*, **125**, 252–278.

Wang, C., S.-K. Lee, and D.B. Enfield, 2008a: Atlantic warm pool acting as a link between Atlantic multidecadal oscillation and Atlantic tropical cyclone activity. Geochemistry Geophysics Geosystems, **9,** Q05V03, doi:10.1029/2007GC001809.

Wang, C., S.-K. Lee, and D.B. Enfield, 2008b: Climate response to anomalously large and small Atlantic warm pools during the summer. *J. Climate*, **21,** 2437-2450.

Warner, T. T., 2010: *Numerical Weather and Climate Prediction*. Cambridge University Press, 548 pp.

Warner, T. T., and H.-M. Hsu, 2000: Nested-Model Simulation of Moist Convection: The Impact of Coarse-Grid Parameterized Convection on Fine-Grid Resolved Convection. *Mon. Wea. Rev.*, **128**, 2211–2231.

Warner, T. T., B. E. Mapes, and M. Xu, 2003: Diurnal Patterns of Rainfall in Northwestern South America. Part II: Model Simulations. *Mon. Wea. Rev.*, **131**, 813–829.

Washington, W. M., and C. L. Parkinson, 2005: *An Introduction To Three-Dimensional Climate Modeling*. University Science Books, 372 pp.

Wilby, R., and C. Dawson, 2007: Using SDSM 4.2- A decision support tool for the assessment of regional climate change impacts. England, UK, 94 pp.

Wilks, D. S., 2005: *Statistical Methods in the Atmospheric Sciences: An Introduction*. 2nd Revised ed. Academic Press Inc, 648 pp.

Whitaker, Jeffrey S., Thomas M. Hamill, Xue Wei, Yucheng Song, Zoltan Toth, 2008: Ensemble Data Assimilation with the NCEP Global Forecast System. *Mon. Wea. Rev.*, **136**, 463–482.

Xiu, A., and J. E. Pleim, 2001: Development of a Land Surface Model. Part I: Application in a Mesoscale Meteorological Model. *J. Appl. Meteor.*, **40**, 192–209.